

Tacrine-sugar mimetic conjugates as enhanced cholinesterase inhibitors†

Quelli Larissa Oliveira de Santana,^{a,b} Tereza C. Santos Evangelista,^{a,b} Petra Imhof,^{1 c} Sabrina Baptista Ferreira,^b José G. Fernández-Bolaños,^d Magne O. Sydnes,^a Óscar Lopéz,^{*d} and Emil Lindbäck,^{*a}

We have used the azide-alkyne Huisgen cycloaddition reaction to obtain two families of bivalent heterodimers where tacrine is connected to an azasugar or iminosugar, respectively, *via* linkers of variable length. The heterodimers were investigated as cholinesterase inhibitors and it was found that their activity increased with the length of the linker. Two of the heterodimers were significantly stronger acetylcholinesterase inhibitors than the monomeric tacrine. Molecular modelling indicated that the longer heterodimers fitted better into the active gorge of acetylcholinesterase than the shorter counterparts and the former provided more efficient simultaneous interaction with the tryptophan residues in the catalytic anionic binding site (CAS) and the peripheral anionic binding site (PAS).

Introduction

Alzheimer's disease (AD) is an age-related progressive neurodegenerative disorder of the brain, which results in death 3–9 years after diagnoses.¹ The anatomical hallmarks of AD include atrophy of regions in the brain, which are associated with cognitive impairment and memory loss.² AD is considered a multifactorial disorder for which the exact pathological mechanisms involved are not fully understood,³ but it is thought to include hallmarks such as formation of beta-amyloid (β A) protein deposits (the major component of extraneuronal senile plaque), accumulation of hyperphosphorylated tau protein (the major component in intracellular neurofibrillary tangles (NFTs)),^{1,4} inflammation,⁵ deficits of the neurotransmitter acetylcholine (ACh),⁶ oxidative stress,⁷ and metal ion dyshomeostasis.⁸

Currently, there is no remedy available for AD,⁹ which is associated with the fact that the causes of the disease have not yet been pinpointed.¹⁰ The best medicinal health care for AD patients at the moment is palliative drugs, in particular acetylcholinesterase inhibitors (AChEIs).³ The first such drug to be

approved for clinical use was tacrine (9-amino-1,2,3,4-tetrahydroacridine) (**1**) (Fig. 1), which was withdrawn from the market as it caused liver damage in *ca.* 30% of the patients.¹¹ The Food and Drug Administration (FDA) has currently four drugs in its arsenal for AD treatment, and three of them, namely donepezil (Aricept®) (**2**), galantamine (Razadyne®) (**3**), and rivastigmine (Exelon®) (**4**) (Fig. 1) are AChEI drugs.¹² The mechanism of action for these drugs is inhibition of the enzyme acetylcholinesterase (AChE) and thereby increasing the neurotransmission, mediated by its substrate acetylcholine (ACh).¹³ Such AD treatment is in line with the cholinergic hypothesis, which suggests that a low level of ACh in the brain is the reason for cognitive declines found in AD patients.¹⁴ In this context, it is worth mentioning that treatment of AD patients with symptomatic relief drugs increase the cost of treatment as they prolong the patients' mild, moderate, and severe stages of the disease,¹⁵ which apart from the personal burden emphasizes the urgent need to develop new drugs to cure AD.

In addition to AChE, butyrylcholinesterase (BuChE) is another type of cholinesterase (ChE), which shares 65% of the amino acid sequence with AChE.¹⁶ However, in a healthy brain, AChE plays a major role in regulating the ACh level.¹⁷ During the progression of AD, the BuChE level in the brain is increased up to 120% and the AChE level is reduced to 55–67% compared to an AD free brain.¹⁸ Thus, cholinesterase inhibitors (ChEIs) such as rivastigmine¹⁹ that exhibit mixed AChE/BuChE inhibition could be beneficial for AD treatment.²⁰ On the other hand, because BuChE exists in low levels in the brain and high levels in peripheral tissues, selective AChE inhibition could be beneficial to avoid side effects.²¹

^aDepartment of Chemistry, Bioscience and Environmental Engineering, Faculty of Science and Technology, University of Stavanger, NO-4036 Stavanger, Norway

^bDepartment of Organic Chemistry, Chemistry Institute, Federal University of Rio de Janeiro, UFRJ, 21949-900 Rio de Janeiro, RJ, Brazil

^cFriedrich-Alexander University (FAU) Erlangen-Nürnberg Computer Chemistry Center, Nügelsbachstrasse 25, 91052 Erlangen, Germany

^dOrgánica, Facultad de Química, Universidad de Sevilla, c/Profesor García González 1, 41012 Seville, Spain

†Electronic supplementary information (ESI) available. See DOI: 10.1039/d0ob02588g

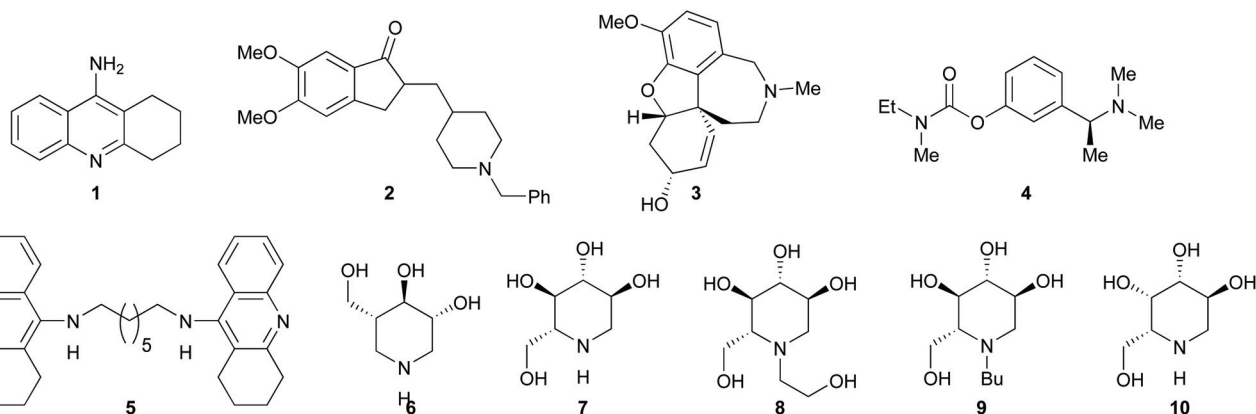


Fig. 1 The structure of cholinesterase inhibitors (ChEIs) 1–5 and glycosidase inhibitors 6–10.

X-ray analysis of *Torpedo californica* acetylcholinesterase (*TcAChE*) revealed a catalytic triad nearby the bottom of a 20 Å deep active gorge decorated with aromatic residues.²² In the proximity of the catalytic triad, a catalytic anionic binding site (CAS) was identified. A second binding site, the peripheral anionic binding site (PAS), that is rich in aromatic residues, was identified at the mouth of the gorge. PAS plays a non-cholinergic function in the progress of AD as it has been found to promote the aggregation of β A protein into amyloid fibrils, which in turn is involved in senile plaque formation.²³ In line with this conclusion, it has been found that AChEIs that bind exclusively to PAS inhibit AChE promoted β A aggregation whereas no such inhibition was observed for the AChEIs that bind exclusively to CAS.²⁴ In addition, dual binding site AChEIs (*i.e.* inhibitors that bind simultaneously to the PAS and CAS) have been found not only to inhibit the hydrolysis of ACh but also AChE promoted aggregation of β A protein,^{24,25} which are both attractive targets for AD treatment.²⁶

X-ray analysis of tacrine in complex with *TcAChE* has shown that tacrine is bound in CAS where it interacts with Trp84 *via* π stacking interactions.²⁷ However, computational studies have shown that tacrine has a low affinity interaction with Trp279 in PAS.²⁸ Indeed, X-ray analysis of bivalent tacrine dimer 5 (bis(7)-tacrine) (Fig. 1) in complex with *TcAChE* revealed a chelation effect in which one of the tacrine rings established interaction with PAS whereas the other tacrine ring interacted with CAS in a very similar way as tacrine bound alone to *TcAChE*.²⁹ Comparison of the ChE inhibitory properties between tacrine homodimer 5 revealed: that 5 is a 1000 times stronger AChEI than tacrine and that 5 is 10 000 times more selective for the inhibition of AChE over BuChE compared to tacrine.³⁰ The significantly higher AChE inhibition activity of 5 was attributed to its interaction with PAS (in addition to CAS), which plays an essential role for the high selectivity for AChE inhibition as BuChE is missing aromatic residues that are present in PAS of AChE.²⁹ The very high AChE inhibition activity by 5 has triggered the synthesis and biological evaluation of other homobivalent^{25c,d,31} and heterobivalent³² tacrine derivatives. An important aspect for such compounds to behave as

efficient dual binding site AChEIs is that the length of the linker between the two binding units is of an optimized length to allow simultaneous interaction with CAS and PAS.³³ In addition, hydrophobic interactions between mid-gorge residues and the linker³⁴ along with the gain in entropy when gorge bound water molecules are replaced by a bound inhibitor^{29,35} contribute to enhanced binding affinity. Tacrine derivatives have not only been found to increase the inhibition potency of AChE, it has also been found that a new series of *N*-propargyl tacrines displays significantly lower hepatotoxicity than tacrine,³⁶ which indicate that the identification of tacrine derivatives as novel AD drugs are of interest.

Azasugars (such as 6 in Fig. 1) and iminosugars (such as 7–10 in Fig. 1) are mostly known for their glycosidase inhibitory potency, which has been attributed to their ability to be protonated at physiological pH and thereby constitute charged analogues of the transition state for enzymatic cleavage of glycosides.³⁷ The inhibition activity of glycosidases by aza- and iminosugars has attracted interest to evaluate them for treatment of disorders such as diabetes, cancer, viral infections, and lysosomal storage disorders.³⁸ To date, three iminosugars, namely, Glyset® (*N*-(2-hydroxyethyl)-1-deoxynojirimycin) (8), Zavesca® (*N*-butyl-1-deoxynojirimycin) (9) and Galafold® (1-deoxygalactonojirimycin) (10) (Fig. 1) are in clinical use for the treatment of type 2 diabetes,³⁹ Gaucher's,⁴⁰ and Fabry's disease,⁴¹ respectively. However, the biological activity of iminosugars goes beyond inhibition of glycosidases. For instance, it was recently found that some iminosugars behave as potent inhibitors of cholinesterases,⁴² although such property has only been scarcely explored. It was proposed that iminosugars in their protonated form, at least to some extent, resemble the charged ChEs substrate ACh,^{42a} which is an important aspect for generating interactions with the active gorge of AChE.²⁷

In this project, we targeted tacrine-isofagomine 12a–12d and tacrine-1-deoxynojirimycin 13a–13c heterodimers (Fig. 2) as potential cholinesterase inhibitors. As mentioned above, the fact that one tacrine moiety in tacrine dimer 5 binds to CAS and the other tacrine moiety binds to PAS demonstrate that tacrine possesses affinity for both binding sites.²⁹ In

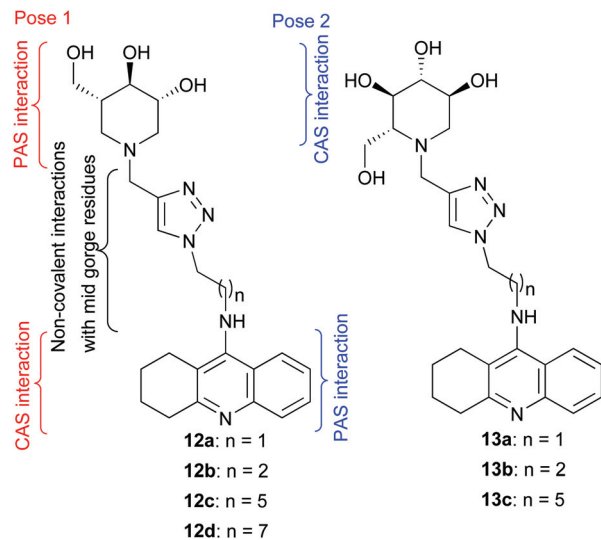


Fig. 2 Compounds **12** and **13** represent the proposed ChEIs in the work presented in this paper.

In addition, the quaternary ammonium groups of decamethonium (DECA) interact simultaneously with Trp279 and Trp84 in PAS and CAS, respectively.²⁷ Because pK_{aH} for isofagomine (**6**) and 1-deoxyojirimycin (DNJ) (**7**) is 8.4⁴³ and 6,7,⁴⁴ respectively, we hypothesize that a significant fraction of **12** and **13** would be protonated on the nitrogen atom of the isofagomine and DNJ moiety, respectively. As such, when the pharmacophores are connected with a linker of optimized length, we argue that **12** and **13** could act as dual binding site AChEIs in two possible general poses (Fig. 2): the sugar mimetic group (isofagomine or DNJ) and tacrine group bound to PAS and CAS (pose 1), respectively, or the opposite way around (pose 2) (Fig. 2). In addition, we envisaged that the connection of the two binding units, namely, isofagomine or deoxyojirimycin with tacrine using Cu(I) catalyzed alkyne-azide cyclization would provide additional interactions with the enzyme, as triazole linkages in other bivalent AChE inhibitors have been found to establish various types of non-covalent interactions with mid gorge residues.⁴⁵

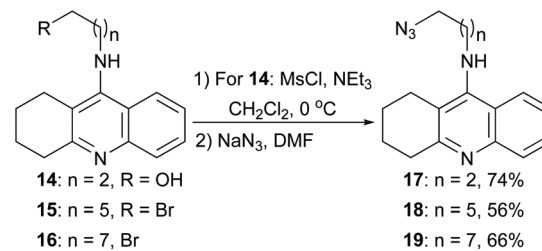
In this paper, we present the synthesis of heterodimers **12** and **13** in which the pharmacophores are connected *via* a linker of variable length, results from biological testing of **12** and **13** as ChEIs, and results from docking studies of **12** and **13** into AChE.

Results and discussion

Synthesis

Azide **17** was obtained from alcohol **14**,⁴⁶ *via* a mesylation-azidation sequence (Scheme 1). Azides **18** and **19** were obtained from alkyl bromide **15** and **16**,⁴⁷ respectively, upon treatment with sodium azide in DMF.

With the azide-armed tacrines **17**, **18**, and **19** in hand, the synthesis of isofagomine-tacrine heterodimers **12a–12d** continued from known nitro alcohol **20**⁴⁸ (Scheme 2), which was sub-



Scheme 1 Synthesis of azidoalkyl-functionalized tacrines **17–19**.

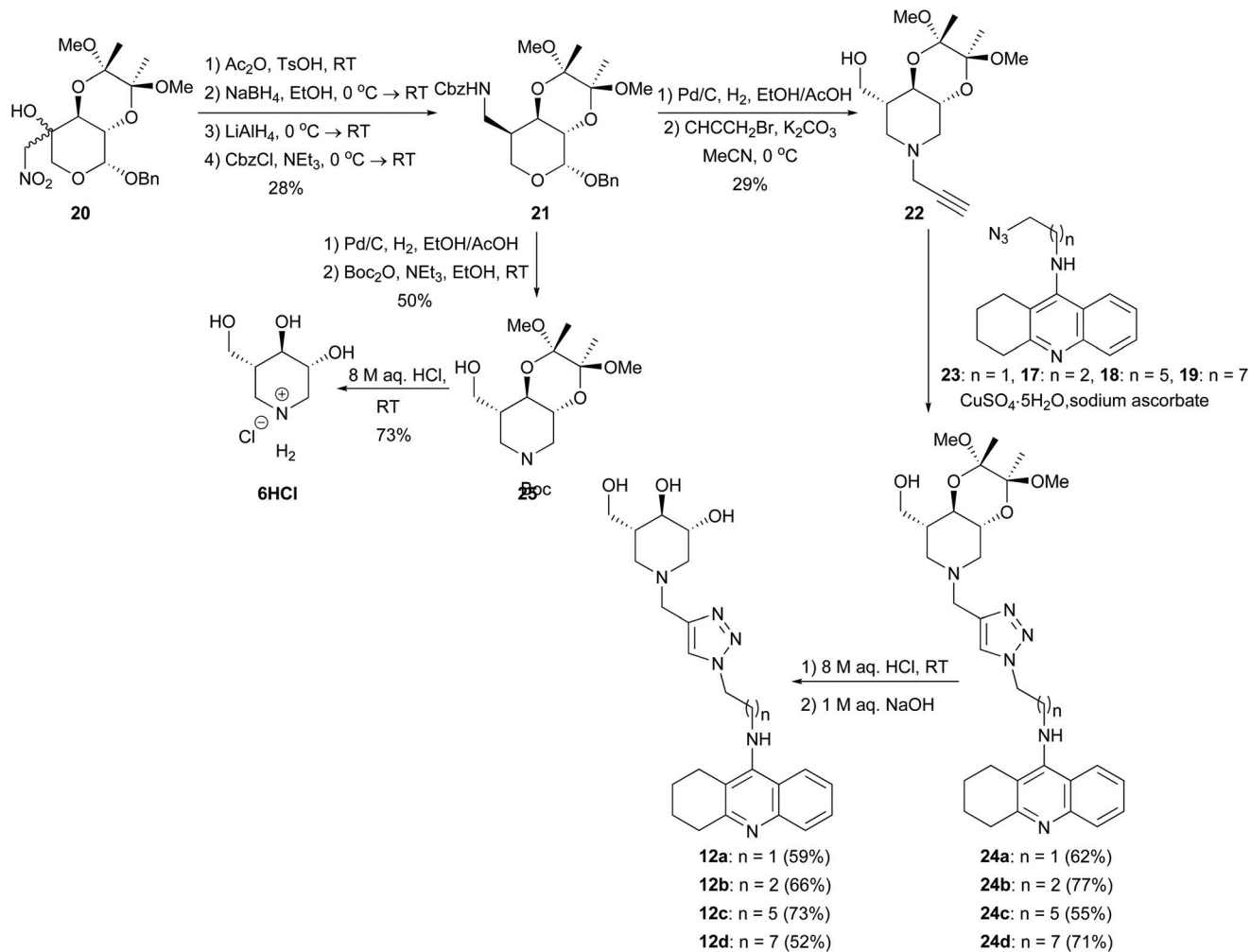
jected to an acetylation-reduction-Cbz protection sequence to provide carbamate **21**. This compound was subjected to palladium-catalyzed hydrogenation followed by propargylation to provide propargylamine **22**. In the following step, this compound was subjected to Cu(I) catalyzed cycloaddition with known azide **23**³⁴ in addition to **17**, **18**, and **19** to provide isofagomine-tacrine heterodimers **24a**, **24b**, **24c**, and **24d**, respectively, in 55–77% yield. In the following step, the acetal ring was removed upon treatment with 8 M aqueous HCl to provide isofagomine-tacrine heterodimers **12a–12d** after treatment with aqueous NaOH. To obtain the hydrochloric acid salt **6HCl** of isofagomine, compound **21** was subjected to palladium-catalyzed hydrogenation followed by Boc-protection (to simplify purification) to obtain carbamate **25**. Treatment of **25** with aqueous HCl provided **6HCl**.

The synthesis of 1-deoxyojirimycin-tacrine heterodimers **13a–13c** started from known alkyne **26**⁴⁹ (Scheme 3). This compound underwent Cu(I) catalyzed cycloaddition with azides **23**, **17**, and **18** to provide heterodimers **27a–27c**. A final BCl₃ promoted *de-O*-benzylation provided the target compounds **13a–13c** after treatment with aqueous NaOH.

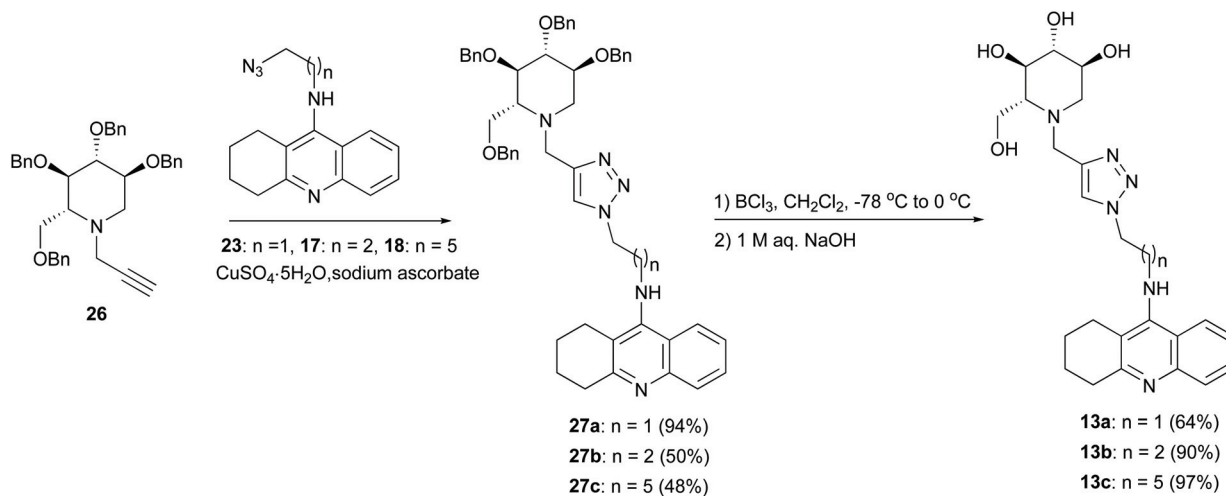
Inhibition studies

Inhibitory properties of derivatives **12a–d** and **13a–c** against cholinesterases (AChE from *Electrophorus electricus* and BuChE from equine serum) were obtained using the Ellman's colorimetric assay (see the Experimental section for details). Data for the anti-Alzheimer's drugs tacrine, donepezil and galantamine, as positive controls, and parent isofagomine-HCl (**6HCl**) and DNJ (**7**) were also included for comparison. The inhibition constants and the mode of inhibition obtained for these compounds are shown in Table 1; the mode of inhibition was double checked using the Cornish-Bowden plots ($1/V$ vs. $[I]$ and $[S]/V$ vs. $[I]$). As an example, Cornish-Bowden plots for the inhibition of AChE by compound **13c** is depicted in Fig. 3.

The data depicted in Table 1 show interesting structure-activity relationships; thus, the absence of the tacrine moiety led to complete lack of activity (entry 8, **6HCl**, $K_i > 100 \mu\text{M}$), or weak inhibitory properties against BuChE (entry 9, DNJ, micromolar range). Although moderate, the latter result confirms that the iminosugar moiety is capable of entering and interacting with cholinesterases, at least with BuChE. In this context, some of us recently reported that some DNJ derivatives armed with electron rich aromatics behaved as good BuChE inhibi-

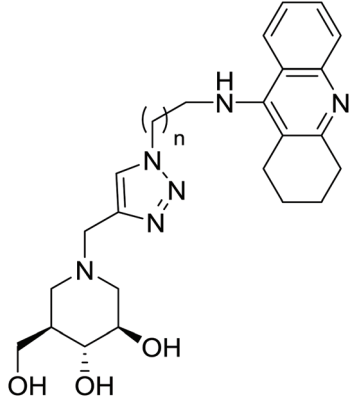
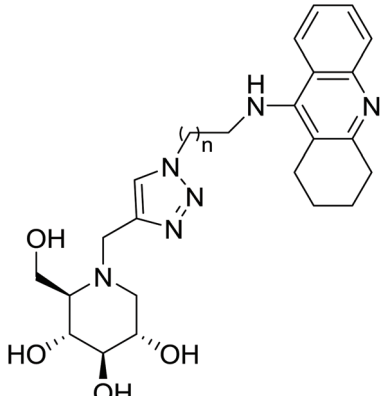


Scheme 2 Synthesis of tacrine-isofagomine heterodimers 12a–12d.



Scheme 3 Synthesis of DNJ-tacrine heterodimers 13a–13c.

Table 1 Inhibitory constants (K_i , μM) and mode of inhibition against *Electrophorus electricus* AChE and equine serum BuChE for derivatives **12a–12d** and **13a–13c**

Entry	Compound	n	AChE	BuChE
				
1	12a	1	$K_{ia} = 2.1 \pm 0.4$ (Competitive)	$K_{ia} = 0.69 \pm 0.13$ $K_{ib} = 0.81 \pm 0.34$ (Mixed)
2	12b	2	$K_{ia} = 1.3 \pm 0.3$ $K_{ib} = 2.7 \pm 0.9$ (Mixed)	$K_{ia} = K_{ib} = 1.5 \pm 0.2$ (Non-competitive)
3	12c	5	$K_{ia} = 0.0289 \pm 0.0094$ $K_{ib} = 0.0302 \pm 0.0058$ (Mixed)	$K_{ia} = 0.26 \pm 0.04$ $K_{ib} = 0.63 \pm 0.18$ (Mixed)
4	12d	7	$K_{ia} = 0.0114 \pm 0.0028$ $K_{ib} = 0.0175 \pm 0.0024$ (Mixed)	$K_{ia} = 0.012 \pm 0.004$ $K_{ib} = 0.030 \pm 0.007$ (Mixed)
				
5	13a	1	$K_{ia} = 3.6 \pm 1.0$ $K_{ib} = 2.3 \pm 0.6$ (Mixed)	$K_{ia} = 1.6 \pm 0.1$ $K_{ib} = 4.8 \pm 0.5$ (Mixed)
6	13b	2	$K_{ia} = 1.8 \pm 0.5$ $K_{ib} = 2.1 \pm 0.1$ (Mixed)	$K_{ia} = 0.45 \pm 0.12$ $K_{ib} = 2.3 \pm 0.9$ (Mixed)
7	13c	5	$K_{ia} = 0.0071 \pm 0.0010$ $K_{ib} = 0.0174 \pm 0.0056$ (Mixed)	$K_{ia} = 0.44 \pm 0.07$ $K_{ib} = 2.1 \pm 0.2$ (Mixed)
8	Isifagomine-HCl (6HCl)		>100	>100
9	DNJ (7)		>100	$K_{ia} = K_{ib} = 16 \pm 3$ (Non-competitive)
10	Tacrine (1)		$K_{ia} = K_{ib} = 0.0548 \pm 0.0039$ (Non-competitive)	$K_{ia} = K_{ib} = 0.0048 \pm 0.0005$ (Non-competitive)
11	Donepezil (2)		$IC_{50} = 0.035^{50}$	$IC_{50} = 2.3^{50}$
12	Galantamine (3)		$K_{ia} = 1.5 \pm 0.6$ (Competitive)	$K_{ia} = 4.5 \pm 0.9$ (Competitive)

tors,^{42c} with activities within the low micromolar range, even stronger than marketed donepezil and galantamine. Molecular docking simulations revealed H-bond interactions between the

minosugar residue and the enzyme catalytic subsite, together with van der Waals interactions involving the aromatic appendage and the PAS region of the enzyme.^{42c}

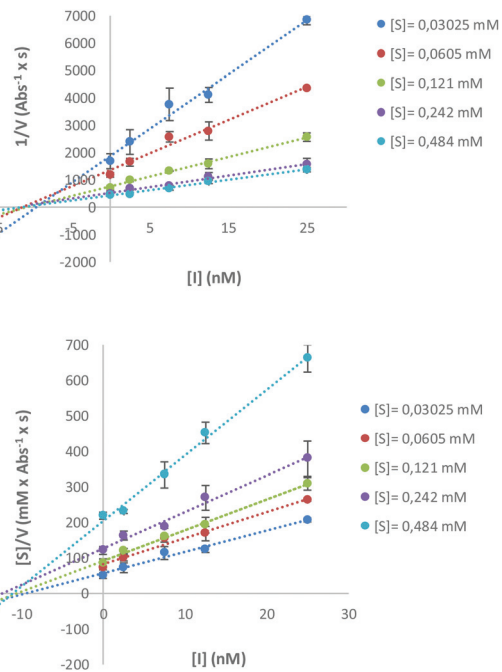


Fig. 3 Cornish-Bowden plots for compound **13c** against AChE (V : rate of reaction, $[S]$: substrate concentration, and $[I]$: inhibitor concentration); errors (SD) for $n = 2$.

Both families of compounds, isofagomine-tacrine heterodimers **12a–12d** (entries 1–4) and DNJ-tacrine heterodimers **13a–13c**, (entries 5–7) presented herein followed the same inhibition profile, namely, that the inhibition activity of both AChE and BuChE increased by the number of methylene groups in the linker between the pharmacophores. However, the trend was more distinctive for the inhibition of AChE; interestingly, and based on the IC_{50} values, a 4 to 6 fold enhancement in activity was achieved for heterodimers **12c** ($IC_{50} = 14.0$ nM), **12d** ($IC_{50} = 11.0$ nM), and **13c** ($IC_{50} = 7.9$ nM) compared to tacrine ($IC_{50} = 50$ nM) against AChE. These results suggest that increasing the length of the linker might allow more efficient simultaneous interaction with PAS and CAS according to pose 1 or pose 2 in Fig. 2. The suggested dual binding site inhibition profile is supported by the mixed inhibition profile of AChE by **12c**, **12d**, and **13c**, which has also been observed for donepezil (**2**)⁵¹ for which X-ray analysis revealed that it binds simultaneously to CAS and PAS of AChE.⁵² Tacrine was found to be a non-competitive inhibitor (special type of mixed inhibition with both inhibitory constants equal to each other), in agreement with previously reported data.⁵³

In this project it is also interesting to note that when tacrine, which is a powerful AChEI, is dimerized with isofago-

display significantly higher inhibition activity than tacrine. Such observations have been made earlier when tacrine heterodimers that are more potent AChEIs than tacrine alone have been obtained by assembling tacrine with a compound that is

a very weak AChEI alone, which demonstrate the power of bivalent AChE inhibition.⁵⁴

Docking and molecular dynamics simulation studies

Docking of the bivalent heterodimers **12a**, **12c**, **13a**, and **13c** to the *Electrophorus electricus* AChE enzyme resulted in relative binding affinities of the respective nine most favorable poses within a range of 1.0 kcal mol⁻¹ for all ligands considered, in both their respective protonation variants, which is protonated at the isofagomine moiety (sugNH) for **12a** and **12c** and the DNJ moiety (sugH) for **13a** and **13c** or at the tacrine moiety (tacNH). Also for each ligand model, there was a pose with the isofagomine moiety (of **12a** and **12c**) or DNJ moiety (of **13a** and **13c**) in contact with PAS and the tacrine moiety in contact with CAS, suggested as pose 1 in Fig. 1, and one with the reverse orientation, namely, the tacrine moiety in contact with the PAS and the isofagomine moiety (of **12a** and **12c**) or DNJ moiety (of **13a** and **13c**) in contact with CAS, termed pose 2 in Fig. 1. The estimated binding affinities differ only marginally between the two poses (0.4 – 1.0 kcal mol⁻¹).

All docking poses (pose 1 or 2) of all investigated ligands (**12a**, **12c**, **13a**, and **13c**), regardless of the length of the linker between the pharmacophores, show the isofagomine or DNJ moiety and the tacrine moiety close to residues Trp86 or Trp286 (*Electrophorus electricus* AChE numbering) in the active gorge, respectively.

However, the longer ligands **12c** and **13c** ($n = 5$), form closer contacts to residues Trp86 and Trp286 than the shorter ($n = 1$) ligands **12a** and **13a**. In the latter cases, the stacking of the moiety in the CAS (tacrine or sugar mimetic, respectively) is wedged between Trp86 and Tyr337, indicating optimal placement, whereas only the tacrine moiety has contact with Trp286 in the PAS, which indicates that the tacrine moiety possesses higher affinity for the Trp residues than the isofagomine moiety and DNJ moiety in **12a** and **13a**, respectively.

Comparison of protonated ligands with the same length and the same pose, but different site of protonation (sugNH or tacNH) and different sugar mimic moiety (isofagomine for **12** or DNJ for **13**), show that the tacrine rings share the same position for the long ligands **12c** and **13c** and in pose 1 are also placed very similarly for the shorter **12a** and **13a** ligands (see Fig. S2†). In pose 2, the tacrine rings of the shorter ligands are slightly closer to Trp286 than those of their longer counterparts.

Representative snapshots from the MD simulations are provided as supplementary material (Fig. S3†). The initial poses are largely maintained throughout the MD simulations, though the actual conformations exhibit some fluctuations. **12c** in pose 2, however, shows its sugar moiety leaving the wedged position between Trp86 and Tyr337, but remaining

and **13a** in pose 1 seem to be less well accommodated in the active gorge of AChE than their longer counterparts **12c** and **13c** in the same pose, which is in agreement with the observation that **12c** ($IC_{50} = 14.0$ nM) is a 24 times stronger AChEI

Table 2 Summed interactions energies (kJ mol^{-1}) of the sugar, tacrine, and triazole moieties of AChEIs **12a**, **12b**, **12c**, and **13d** with the AChE enzyme (sugNH = isofagomine moiety for **12a** and **12c** or DNJ moiety of **13a** and **13c**; TacNH = tacrine moiety; pose 1 and pose 2 refer to figure)

Compound	12a		13a		12c		13c	
Protonation	sugNH	tacNH	sugNH	tacNH	sugNH	tacNH	sugNH	tacNH
Pose 1	-411.1 ± 3.2	-401.7 ± 5.5	-464.5 ± 27.2	-413.1 ± 10.0	-477.8 ± 10.9	-413.3 ± 11.8	-517.0 ± 5.0	-372.3 ± 5.5
Pose 2	-458.5 ± 1.5	-437.4 ± 5.5	-419.0 ± 3.9	-426.6 ± 4.1	-332.9 ± 25.6	-317.4 ± 9.6	-493.2 ± 19.6	-422.0 ± 14.3

than **12a** ($\text{IC}_{50} = 340 \text{ nM}$) and **13c** ($\text{IC}_{50} = 7.9 \text{ nM}$) a 190 times stronger AChEI than **13a** ($\text{IC}_{50} = 1500 \text{ nM}$). We have computed interaction energies between AChEIs **12a**, **12c**, **13a** or **13c** with the AChE enzyme. Comparison of those interaction energies (Table 2) reveals sugar mimetic protonated (sugNH) ligands exhibit stronger interactions with the enzyme than their tacrine-protonated (tacNH) counterparts in the same pose, with the exception of **13a** in pose 2 where the tacrine protonated moiety (tacNH) is slightly preferred. Of all models with **12a**, **12c**, **13a**, or **13c** in complex with AChE, sugar mimetic protonated **13c** interacts most favorably with the protein when in pose 1 (Fig. 4a), that is with its DNJ moiety at the PAS and the tacrine moiety positioned in the CAS, and still considerably strong when in pose 2 (Fig. 4b). Thus, both the relative interaction energies and the MD simulations are in agreement with the fact that **13c** is a more potent AChEI than **12a**, **12c**, and **13a**.

Interaction energies calculated for the shorter ligands **12a** and **13a** (Table 2) indicate preferential binding to the active gorge of AChE in pose 2 and pose 1, respectively, in which the both ligands are protonated at the sugar mimetic moiety.

For ligand **12c**, pose 1 is favored over pose 2, as far as interaction energies are concerned, in which **12c** prefers to be pro-

tonated at the isofagomine moiety (sugNH) (-478 kJ mol^{-1}) over the tacrine moiety (tacNH) (-413 kJ mol^{-1}). Indeed, this model, when the isofagomine moiety of AChEI **12c** is protonated in pose 1 shows interaction energies with the AChE enzyme, which within errors come close to that of ligand **13c** in the opposite, less favorable, pose 2. The same holds for the interaction energies of the most favorable model of **13a**, also in pose 1, if one takes the errors in favor of **13a** and in disfavor of **13c** (in pose 2). In other words, even when bound in the “wrong” direction, **13c** is still as strong a binder as the other ligands. When in its preferred pose 1, though, **13c** shows interaction energies with the AChE enzyme that outperform all other ligands in all poses and protonation states, in agreement with the measured considerably higher inhibition activity of this ligand.

Conclusions

Four tacrine-isofagomine and three tacrine-DNJ heterodimers have been synthesized using click-ligation and evaluated as ChEIs as a novel family of potential Alzheimer’s agents. Three of them **12c**, **12d**, and **13c** outperformed the reference compounds tacrine (**1**), donepezil (**2**), and galantamine (**3**) as AChEIs of which **12d** also was a slightly stronger BuChE inhibitor than tacrine, which indicate that both the isofagomine and DNJ moieties contribute with productive interactions to AChE. The observed tendency for the AChE inhibition was that the activity was improved upon increasing the length of the linker between the pharmacophores, which was expected to be crucial for simultaneous interaction with PAS and CAS. In fact, modelling studies indicated that the longer ligands **12c** and **13c** interact more favorably into the active gorge than the shorter counterparts **12a** and **13a**, respectively. An interesting observation was that the tacrine moiety could be in either CAS or PAS depending on the identity of the sugar mimetic moiety in the heterodimers. Our data suggest that for the stronger binders, *i.e.* the longer ligands, binding of the tacrine moiety to CAS is preferred (defined as pose 1 in Fig. 2).

Experimental

General experimental

Dichloromethane was dried over 4 \AA molecular sieves (oven dried). For petroleum ether (PE), the 40–65 °C fraction was used. All reactions were carried out under a N_2 or Ar atmosphere if not otherwise specified. TLC analyses were per-

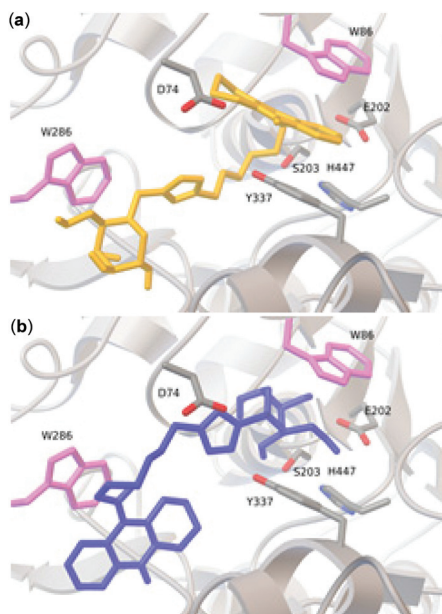


Fig. 4 Ligand **13c** interacts more efficiently with AChE in pose 1 (a) compared to pose 2 (b) (pose 1 and pose 2 are defined in Fig. 2).

formed on Merck silica gel 60 F254 plates using UV light for detection. Silica gel NORMASIL 60® 40–63 μm was used for flash column chromatography. NMR spectra were recorded with a Bruker Avance NMR spectrometer; ¹H NMR and ¹³C NMR spectra were recorded at 400.13 MHz and 100.61 MHz, respectively. Chemical shifts are reported in ppm relative to an internal standard of residual chloroform (δ = 7.26 ppm for ¹H NMR; δ = 77.00 ppm for ¹³C NMR), residual methanol (δ = 3.31 ppm for ¹H NMR; δ = 49.00 ppm for ¹³C NMR). High-resolution mass spectra (HRMS) were recorded from MeOH solutions on a JMS-T100LC AccuTOFTM in positive electro-spray ionization (ESI) mode.

Synthetic procedures

***N*-(3-Azidopropyl)-1,2,3,4-tetrahydroacridin-9-amine (17).** To a suspension of alcohol **14** (497 mg, 1.94 mmol, 1 equiv.) and NEt₃ (0.31 mL, 2.21 mmol, 1.15 equiv.) in anhydrous CH₂Cl₂ (12 mL) at 0 °C under a N₂-atmosphere was added dropwise MsCl (0.16 mL, 2.08 mmol, 1.07 equiv.). After addition, the mixture was kept stirring for 15 minutes before the addition of saturated aqueous NaHCO₃ (15 mL) and CH₂Cl₂ (15 mL). The layers were separated, and the organic layer was dried (MgSO₄), filtered, and concentrated under reduced pressure. The crude mesylate was dissolved in DMF (4 mL) and to the solution was added NaN₃ (505 mg, 7.76 mmol, 4 equiv.). After addition, the mixture was kept stirring at 45 °C overnight. Saturated aqueous NaCl (20 mL) and EtOAc (20 mL) were added and the organic layer was collected and concentrated under reduced pressure. Purification of the residue by silica gel flash column chromatography (CHCl₃/MeOH/NH₄OH 475 : 25 : 1) provided the title compound **17** (404 mg, 74%) as a yellow oil. *R*_f 0.42 (CHCl₃/MeOH/NH₄OH 475 : 25 : 1); ¹H-NMR δ_H (CDCl₃, 400.13 MHz) 7.93–7.91 (2 H, m, ArH), 7.58–7.54 (2 H, m, ArH), 7.39–7.35 (1 H, m, ArH), 4.07 (1 H, brs, NH), 3.57 (2 H, t, *J* = 6.5 Hz, CH₂), 3.46 (2 H, t, *J* = 6.4 Hz, CH₂), 3.08–3.06 (2 H, m, CH₂), 2.75–2.72 (2 H, m, CH₂), 1.96–1.89 (2 H, m, 3 × CH₂); ¹³C-NMR δ_C (CDCl₃, 100.61 MHz) 158.8 (Ar), 150.3 (Ar), 147.5 (Ar), 129.0 (Ar), 128.6 (Ar), 124.2 (Ar), 122.5 (Ar), 120.6 (Ar), 117.1 (Ar), 49.5 (CH₂), 46.8 (CH₂), 34.1 (CH₂), 30.7 (CH₂), 25.1 (CH₂), 23.2 (CH₂), 22.9 (CH₂); HRMS (ESI); calcd for C₁₆H₂₀N₅⁺ 282.1713; found 282.1711.

General procedure for the preparation of compounds 18 and 19. To a solution of the alkyl bromide **15** or **16** (2.40 mmol, 1 equiv.) in DMF (10 mL) was added NaN₃ (9.60 mmol, 4 equiv.). The mixture was heated overnight at 80 °C under Ar-atmosphere. After this time, the mixture was cooled to room temperature and the solvent was evaporated under reduced pressure. Then, 100 mL of water was added, and the aqueous phase was extracted with EtOAc (2 × 100 mL). The phases were separated, and the organic layer was dried with MgSO₄, filtered and concentrated under reduced pressure. The concentrate was purified by silica gel flash column chromatography.

***N*-(6-Azidoheptyl)-1,2,3,4-tetrahydroacridin-9-amine (18).** The crude product of **18** was purified by silica gel flash column chromatography (CH₂Cl₂/MeOH 99 : 1 → 98 : 2 → 95 : 5) to provide **18** (436.1 mg, 56%) as a brown oil. *R*_f 0.60 (CH₂Cl₂/

MeOH/NH₄OH 9 : 1 : 0.1); ¹H-NMR δ_H (CDCl₃, 400.13 MHz) 8.22 (1 H, d, *J* = 8.1 Hz, ArH), 8.09 (1 H, d, *J* = 8.7 Hz, ArH), 7.61–7.57 (1 H, m, ArH), 7.40–7.36 (1 H, m, ArH), 5.18 (1 H, brs, NH), 3.75–3.70 (2 H, m, CH₂), 3.25 (2 H, t, *J* = 6.8 Hz, CH₂), 3.18–3.15 (2 H, m, CH₂), 2.69–2.66 (2 H, m, CH₂), 1.90–1.88 (2 H, m, 2 × CH₂), 1.79–1.74 (2 H, m, CH₂), 1.63–1.56 (2 H, m, CH₂), 1.44–1.40 (4 H, m, 2 × CH₂); ¹³C-NMR δ_C (CDCl₃, 100.61 MHz) 154.7 (Ar), 153.4 (Ar), 142.9 (Ar), 130.5 (Ar), 124.6 (2 × Ar), 123.8 (Ar), 118.0 (Ar), 113.4 (Ar), 51.3 (CH₂), 48.9 (CH₂), 31.4 (CH₂), 31.1 (CH₂), 28.8 (CH₂), 26.5 (2 × CH₂), 24.4 (CH₂), 22.5 (CH₂), 21.7 (CH₂); HRMS (ESI); calcd for C₁₉H₂₆N₅⁺ 324.2183; found 324.2179.

***N*-(8-Azidoheptyl)-1,2,3,4-tetrahydroacridin-9-amine (19).** The crude product of **19** was purified by silica gel flash column chromatography (CH₂Cl₂/MeOH 99 : 1 → 98 : 2 → 95 : 5) to provide **19** (568.1 mg, 66%) as a brown oil. *R*_f 0.64 (CH₂Cl₂/MeOH/NH₄OH 9 : 1 : 0.1); ¹H-NMR δ_H (CDCl₃, 400.13 MHz) 8.07 (1 H, d, *J* = 8.4, ArH), 8.01–7.99 (1 H, m, ArH), 7.60–7.55 (1 H, m, ArH), 7.38–7.34 (1 H, m, ArH), 4.38 (1 H, brs, NH), 3.61–3.56 (2 H, m, CH₂), 3.24 (1 H, t, *J* = 6.8 Hz, CH₂), 3.12 (2 H, brs, CH₂), 2.68–2.66 (2 H, m, CH₂), 1.92–1.88 (4 H, m, 2 × CH₂), 1.73–1.66 (2 H, m, CH₂), 1.60–1.54 (2 H, m, CH₂), 1.42–1.33 (8 H, m, 4 × CH₂); ¹³C-NMR δ_C (CDCl₃, 100.61 MHz) 156.9 (Ar), 152.0 (Ar), 145.5 (Ar), 129.4 (Ar), 127.0 (Ar), 124.1 (Ar), 123.3 (Ar), 119.2 (Ar), 114.7 (Ar), 51.5 (CH₂), 49.4 (CH₂), 32.8 (CH₂), 31.7 (CH₂), 29.3 (CH₂), 29.1 (CH₂), 28.9 (CH₂), 26.9 (CH₂), 26.7 (CH₂), 24.6 (CH₂), 22.9 (CH₂), 22.4 (CH₂); HRMS (ESI); calcd for C₂₁H₃₀N₅⁺ 352.2496; found 352.2488.

Benzyl 4-(benzyloxycarbonyl)aminomethyl-((2′S,3′S)-2′,3′-dimethoxybutan-2′,3′-diyl)-β-D-arabinopyranoside (21). **Step 1:** A mixture of alcohol **20** (1.26 g, 3.05 mmol, 1 equiv.) and *p*-toluenesulfonic acid monohydrate (58.0 mg, 0.305 mmol, 0.10 equiv.) in Ac₂O (12 mL) was stirred overnight at room temperature. Before the solvent was removed under reduced pressure at 30 °C. The concentrate was dissolved in CH₂Cl₂ (100 mL) and saturated aqueous NaHCO₃ (50 mL) was added. The layers were separated, and the organic extract was dried (MgSO₄), filtered, and concentrated under reduced pressure. **Step 2:** The residue was dissolved in EtOH (50 mL) and was added a suspension of NaBH₄ (138.5 mg, 3.66 mmol, 1.2 equiv.) in EtOH (17 mL) at 0 °C under a N₂-atmosphere. After addition, the mixture was kept stirring at room temperature for 90 minutes. The volatiles were removed under reduced pressure and the residue was dissolved in 0.6 M aqueous HCl (50 mL) and EtOAc (50 mL) at 0 °C. The layers were separated, and the organic extract was dried (MgSO₄), filtered, and concentrated under reduced pressure. The residue was dissolved in toluene (×2) and concentrated under reduced pressure. **Step 3:** The concentrate was dissolved in anhydrous THF (37 mL) under a N₂-atmosphere at 0 °C. Then, the solution was added LiAlH₄ (463 mg, 12.2 mmol, 4 equiv.) was then added in portions. After addition, the mixture was allowed to reach room temperature overnight. The reaction was quenched by slow addition of EtOH at 0 °C. After quenching, the mixture was filtered through Celite by the aid of CH₂Cl₂. The filtrate was added H₂O and the phases were separated. The organic layer

1 was dried (MgSO₄), filtered, and concentrated under reduced
pressure. **Step 4:** The residue was dissolved in anhydrous
CH₂Cl₂ (12 mL) and was added anhydrous NEt₃ (0.51 mL,
3.66 mol, 1.2 equiv.) at 0 °C under a N₂-atmosphere. The solu-
5 tion was added dropwise CbzCl (0.43 mL, 3.05 mmol, 1 equiv.)
and the obtained mixture was kept stirring overnight at room
temperature. The volatiles were removed under reduced
pressure and the residue underwent purification by silica gel
column chromatography (EtOAc/PE 17:3 → 4:1) to provide
10 the title compound **21** (432.4 mg, 28%) as a white foam. *R*_f
0.54 (EtOAc/PE 3:7); [α]_D²⁸ +3 (c 0.71, CHCl₃); ¹H-NMR δ_H
(CDCl₃, 400.13 MHz) 7.42–7.27 (10 H, m, ArH), 5.33 (1 H, brs,
NH), 5.11 (2 H, brs, CH₂Ph), 4.88 (1 H, d, *J* = 3.9 Hz, 1-H), 4.73
15 (1 H, d, *J* = 13.0 Hz, CHaPh), 4.65 (1 H, d, *J* = 13.0 Hz, CHbPh),
4.32 (1 H, dd, *J*_{3;4} = 5.5 Hz, *J*_{3;2} = 10.7 Hz, 3-H), 3.93–3.87 (2 H,
m, 2-H, 5a-H), 3.56–3.50 (3 H, m, CH₂N, 5b-H), 3.25 (3 H, s,
OCH₃), 3.20 (3 H, s, OCH₃), 2.03–2.01 (1 H, m, 4-H), 1.32 (3 H,
s, CH₃), 1.27 (3 H, s, CH₃); ¹³C-NMR δ_C (D₂O, 100.61 MHz)
20 156.7 (C=O), 137.8 (2 × Ar), 136.9 (Ar), 128.6–127.6 (5 × Ar),
100.1, 99.9 (2'-C, 3'-C), 96.8 (1-C), 69.2 (CH₂Ph), 66.6 (CH₂Ph),
66.1 (2-C), 65.7 (3-C), 61.1 (5-C), 48.0, 47.9 (OCH₃), 39.7 (4-C),
39.3 (CH₂N), 18.0, 17.8 (2 × CH₃); HRMS (ESI); calcd for
C₂₇H₃₅O₈NNa⁺ 524.2255; found 524.2245.

N-Propargyl-((2',3',3'-dimethoxybutan-2',3'-diyl)isofagomine
(**22**). **Step 1:** A suspension of carbamate **21** (121 mg,
0.243 mmol, 1 equiv.) and Pd/C (10 wt%, 242 mg) in EtOH/
AcOH (9:1; 15 mL) under a N₂-atmosphere was degassed and
introduced a H₂-atmosphere (1 atm). The mixture was kept
stirring overnight. The reaction mixture was then filtered
through Celite® by the aid of EtOH and the filtrate was con-
centrated under reduced pressure. The concentrate was dis-
solved in toluene (×2) and concentrated under reduced
pressure. **Step 2:** The residue was dissolved in anhydrous
MeCN (1.4 mL) under a N₂-atmosphere. K₂CO₃ (67.2 mg,
0.486 mmol, 2 equiv.) was added and the temperature was
adjusted to 0 °C. Propargyl bromide (80 wt% in toluene, 32 μL,
0.486 mmol, 2 equiv.) was then added dropwise and the
mixture was kept stirring at 0 °C for 2 hours and 10 minutes.
Aqueous Na₂S₂O₃ (10 wt%, 10 mL) was then added and the
aqueous mixture was extracted with CH₂Cl₂ (2 × 15 mL). The
phases were separated, and the organic extract was concen-
trated under reduced pressure. Purification of the concentrate
35 by silica column chromatography (EtOAc/PE 1:1 → 3:2) pro-
vided the title compound **22** (21 mg, 29%) as a colorless syrup.
*R*_f 0.50 (EtOAc); [α]_D²⁷ +161 (c 0.36, CHCl₃); ¹H-NMR δ_H
(CDCl₃, 400.13 MHz) 3.85–3.76 (2 H, m, 3-H, CHaOH), 3.63–3.60 (1 H,
m, CHbOH), 3.49–3.44 (1 H, m, 4-H), 3.38 (2 H, d, *J* = 2.2,
CH₂N), 3.28 (3 H, s, OCH₃), 3.27 (3 H, s, OCH₃), 2.89–2.83 (2
40 H, m, 2a-H, 6a-H), 2.37 (1 H, t, *J* = 10.4, *J* = 10.4, 2b-H), 2.26 (1
H, t, *J* = 2.2, CH-alkyne), 2.19–2.08 (2 H, m, 5-H, 6b-H), 1.32 (3
H, s, OCH₃), 1.29 (3 H, s, OCH₃); ¹³C-NMR δ_C (CDCl₃,
100.61 MHz) 100.1, 99.6 (2'-C, 3'-C), 78.1 (C-alkyne), 74.1, 74.0
45 (4-C, CH-alkyne), 68.1 (3-C), 63.9 (CH₂OH), 54.0, 53.4 (2-C,
6-C), 48.1, 48.0 (OCH₃), 46.7 (CH₂N), 40.8 (C-5), 18.1, 17.9
(CH₃); HRMS (ESI); calcd for C₁₅H₂₆NO₅⁺ 300.1805; found
300.1804.

General procedure for the preparation of compounds 24a–
24d. A mixture of alkyne **22** (0.08 M, 1 equiv.), azide **17**, **18**, **19**
or **23** (0.08 M, 1 equiv.), and copper(II) sulfate pentahydrate
(0.3 equiv.) in DMAc (for **24a**, **24c**, and **24d**) or DMF (for **24b**)
in a foil covered round bottom flask was degassed and intro-
5 duced a N₂-atmosphere before the addition of sodium ascor-
bate (0.60 equiv.). The mixture was kept stirring at room temp-
erature for 2.5 hours. The solvent was then removed under
reduced pressure and the concentrate was purified by silica gel
column chromatography.

**N-((1-(2-((1,2,3,4-Tetrahydroacridin-9-yl)amino)ethyl)-1*H*-1,2,3-
triazol-4-yl)methyl)-((2',3',3'-dimethoxybutan-2',3'-diyl)isofa-
gomine (24a).** The crude product of **24a** was purified by silica
gel flash column chromatography (CH₂Cl₂/MeOH/NH₄OH
950:50:1 → 925:75:1 → 900:100:1) to provide **24a**
15 (28.3 mg, 62%) as a light yellow solid. *R*_f 0.20 (CH₂Cl₂/MeOH/
NH₄OH 850:150:1); [α]_D²⁷ +86 (c 0.28, CHCl₃); HRMS (ESI);
¹H-NMR δ_H (CDCl₃, 400.13 MHz) 7.91 (1 H, d, *J* = 8.1 Hz, ArH),
7.78 (1 H, d, *J* = 8.0 Hz, ArH), 7.56–7.52 (1 H, m, ArH), 7.41 (1
20 H, s, ArH), 7.36–7.31 (1 H, m, ArH), 4.55 (2 H, t, *J* = 5.4 Hz,
CH₂), 4.04 (2 H, t, *J* = 4.9 Hz, CH₂), 3.80–3.67 (4 H, m, CH₂-N,
CHaOH, 3-H), 3.54 (1 H, dd, *J*_{CHbOH;5} = 5.1 Hz, *J*_{CHbOH;CHaOH} =
10.9 Hz, CHbOH), 3.39 (1 H, t, *J*_{4;5} = 10.1 Hz, 4-H), 3.23 (3 H, s,
OCH₃), 3.21 (3 H, s, OCH₃), 3.05 (2 H, t, *J* = 6.0 Hz, CH₂),
2.93–2.89 (2 H, m, 2a-H, 6a-H), 2.62 (2 H, t, *J* = 5.9 Hz, CH₂), 2.12
25 (1 H, t, *J*_{2b;2a} = 10.6 Hz, 2b-H), 2.03–1.96 (1 H, m, 5-H), 1.93–1.87
(5 H, m, 6b-H, 2 × CH₂), 1.29 (3 H, s, CH₃), 1.25 (3 H, s, CH₃);
¹³C-NMR δ_C (CDCl₃, 100.61 MHz) 158.2 (Ar), 149.9 (Ar), 146.2
(Ar), 144.4 (Ar), 129.0 (Ar), 128.0 (Ar), 124.6 (Ar), 123.7 (Ar), 122.3
30 (Ar), 120.2 (Ar), 117.5 (Ar), 100.0, 99.5 (2'-C, 3'-C), 74.0 (4-C), 68.1
(3-C), 63.5 (CH₂OH), 55.1 (2-C), 54.1 (6-C), 52.7 (CH₂-N), 50.8
(CH₂), 48.1 (CH₂), 47.9 (OCH₃), 47.8 (OCH₃), 40.9 (5-C), 33.4
(CH₂), 24.9 (CH₂), 22.9 (CH₂), 22.6 (CH₂), 18.0 (CH₃), 17.9 (CH₃);
calcd for C₃₀H₄₃N₆O₅⁺ 567.3289; found 567.3284.

**N-((1-(2-((1,2,3,4-Tetrahydroacridin-9-yl)amino)propyl)-1*H*-1,2,3-
triazol-4-yl)methyl)-((2',3',3'-dimethoxybutan-2',3'-diyl)isofa-
gomine (24b).** The crude product of **24b** was purified by silica
gel flash column chromatography (CH₂Cl₂/MeOH/NH₄OH
925:75:1 → 925:75:3 → 900:100:3) to provide **24b**
40 (83.3 mg, 77%) as a colorless wax. *R*_f 0.16 (CH₂Cl₂/MeOH/
NH₄OH 850:150:3); [α]_D²⁶ +75 (c 0.59, EtOAc); ¹H-NMR δ_H
(400 MHz, CDCl₃) 7.92–7.88 (2 H, m, ArH), 7.57–7.53 (1 H, m,
ArH), 7.38–7.34 (2 H, m, ArH), 4.44 (2 H, t, *J* = 6.6 Hz, CH₂),
4.36 (1 H, brs, NH), 3.81–3.67 (4 H, m, CH₂-N, 3-H, CHaOH),
3.54 (1 H, dd, *J* = 5.0 Hz, *J* = 10.8 Hz, CHbOH), 3.46 (2 H, t, *J* =
6.6 Hz, CH₂), 3.42–3.37 (1 H, m, 4-H), 3.23 (3 H, s, OCH₃), 3.22
45 (3 H, s, OCH₃), 3.06–3.04 (2 H, m, CH₂), 2.93–2.88 (2 H, m, 2a-
H, 6a-H), 2.73 (2 H, brs, CH₂), 2.44 (1 H, brs, OH), 2.24–2.21 (2
50 H, m, CH₂), 2.11 (1 H, t, *J* = 10.5 Hz, 2b-H), 2.05–1.97 (1 H, m,
5-H), 1.91–1.90 (5 H, m, 6b-H, 2 × CH₂), 1.29 (3 H, s, CH₃), 1.25
(3 H, s, CH₃); ¹³C-NMR δ_C (100 MHz, CDCl₃) 158.7 (Ar), 150.2
(Ar), 147.1 (Ar), 144.3 (Ar), 128.8 (Ar), 128.7 (Ar), 124.4 (Ar),
122.9 (Ar), 122.3 (Ar), 120.5 (Ar), 117.2 (Ar), 100.0, 99.6 (2'-C, 3'-
55 C) 74.1 (4-C), 68.1 (3-C), 63.6 (CH₂OH), 55.0 (2-C), 54.2 (6-C),
52.8 (CH₂-N), 48.1 (OCH₃), 48.0 (OCH₃), 47.7 (CH₂), 45.4 (CH₂),
40.9 (5-C), 33.9 (CH₂), 31.7 (CH₂), 25.1 (CH₂), 23.1 (CH₂), 22.8

(CH₂), 18.0 (CH₃), 17.9 (CH₃); HRMS (ESI); calcd for C₃₁H₄₅N₆O₅⁺ 581.3446; found 581.3440.

N-((1-(2-((1,2,3,4-Tetrahydroacridin-9-yl)amino)hexyl)-1*H*-1,2,3-triazol-4-yl)methyl)-((2'*S*,3'*S*)-2',3'-dimethoxybutan-2',3'-diyl)isofagomine (**24c**). The crude product of **24c** was purified by silica gel flash column chromatography (CH₂Cl₂/MeOH/NH₄OH 925:75:1 → 1850:150:3 → 1800:200:3) to provide **24c** (56 mg 55%) as a white foam. *R*_f 0.52 (CH₂Cl₂/MeOH 7:1 + 1 droplet of NH₄OH); [α]_D²⁶ +75 (*c* 0.32, CH₂Cl₂); ¹H-NMR δ_H (CDCl₃, 400.13 MHz) 8.27 (1 H, d, *J* = 7.7 Hz, ArH), 8.07 (1 H, d, *J* = 8.5 Hz, ArH), 7.62 (1 H, t, *J* = 7.3 Hz, ArH), 7.45 (1 H, s, ArH), 7.41–7.37 (1 H, m, ArH), 4.34 (2 H, t, *J* = 7.0 Hz, CH₂), 3.83–3.68 (6 H, m, CH₂-N, CHaOH, CH₂, 3-H), 3.55 (1 H, dd, *J*_{CHbOH;5} = 5.0 Hz, *J*_{CHbOH;CHaOH} = 10.8 Hz, CHbOH), 3.41 (1 H, t, *J*_{4;5} = 10.1 Hz, 4-H), 3.24 (3 H, s, OCH₃), 3.23 (3 H, s, OCH₃), 3.19 (2 H, t, *J* = 5.6 Hz, CH₂), 2.96–2.92 (2 H, m, 2a-H, 6a-H), 2.64 (2 H, t, *J* = 5.7 Hz, CH₂), 2.13 (1 H, t, *J*_{2b;2a} = 10.5 Hz, 2b-H), 2.06–1.98 (1H, m, 5-H), 1.97–1.87 (7 H, m, 6b-H, 3 × CH₂), 1.79–1.72 (2 H, m, CH₂), 1.51–1.44 (2 H, m, CH₂), 1.40–1.35 (2 H, m, CH₂), 1.30 (3 H, s, CH₃), 1.26 (3 H, s, CH₃); ¹³C-NMR δ_C (CDCl₃, 100.61 MHz) 154.7 (Ar), 153.8 (Ar), 144.1 (Ar), 130.9 (Ar), 124.9 (Ar), 123.8 (Ar), 122.8 (Ar), 114.4 (Ar), 100.1, 99.7 (2'-C, 3'-C), 74.2 (4-C), 68.2 (3-C), 63.7 (CH₂OH), 55.2 (2-C), 54.1 (6-C), 52.9 (CH₂-N), 50.1 (CH₂), 48.8 (CH₂), 48.2 (OCH₃), 48.1 (OCH₃), 41.0 (5-C), 31.3 (CH₂), 30.8 (CH₂), 30.2 (CH₂), 26.3 (CH₂), 26.2 (CH₂), 24.4 (CH₂), 22.6 (CH₂), 21.7 (CH₂), 18.1 (CH₃), 18.0 (CH₃) (three aromatic carbons are obscured or overlapping); HRMS (ESI); calcd for C₃₄H₅₁N₆O₅⁺ 623.3915; found 623.3906.

N-((1-(2-((1,2,3,4-Tetrahydroacridin-9-yl)amino)octyl)-1*H*-1,2,3-triazol-4-yl)methyl)-((2'*S*,3'*S*)-2',3'-dimethoxybutan-2',3'-diyl)isofagomine (**24d**). The crude product of **24d** was purified by silica gel flash column chromatography (CH₂Cl₂/MeOH/NH₄OH 925:75:1 → 1850:150:3 → 1800:200:3) to provide **24d** (36.5 mg, 71%). *R*_f 0.56 (CH₂Cl₂/MeOH 7:1 + 1 droplet of NH₄OH); [α]_D²⁶ +73 (*c* 0.52, CH₂Cl₂); ¹H-NMR δ_H (CDCl₃, 400.13 MHz) 8.12 (1 H, d, *J* = 8.4 Hz, ArH), 8.03 (1 H, d, *J* = 8.5 Hz, ArH), 7.58 (1 H, t, *J* = 7.3 Hz, ArH), 7.42 (1 H, s, ArH), 7.37 (1 H, t, *J* = 7.3 Hz, ArH), 4.30 (2 H, t, *J* = 7.2 Hz, CH₂), 3.82–3.67 (4 H, m, CH₂-N, CHaOH, 3-H), 3.63 (2 H, t, *J* = 7.2 Hz, CH₂), 3.54 (1 H, dd, *J*_{CHbOH;5} = 5.0 Hz, *J*_{CHbOH;CHaOH} = 10.8 Hz, CHbOH), 3.40 (1 H, t, *J*_{4;5} = 10.1 Hz, 4-H), 3.23 (3 H, s, OCH₃), 3.22 (3 H, s, OCH₃), 3.13 (2 H, t, *J* = 5.5 Hz, CH₂), 2.94–2.89 (2 H, m, 2a-H, 6a-H), 2.65 (2 H, t, *J* = 5.7 Hz, CH₂), 2.11 (1 H, t, *J*_{2b;2a} = 10.6 Hz, 2b-H), 2.05–1.98 (1 H, m, 5-H), 1.93–1.86 (7 H, m, 6b-H, 3 × CH₂), 1.73–1.66 (2 H, m, CH₂), 1.41–1.31 (8 H, m, 4 × CH₂), 1.29 (3 H, s, CH₃), 1.25 (3 H, s, CH₃); ¹³C-NMR δ_C (CDCl₃, 100.61 MHz) 155.8 (Ar), 152.8 (Ar), 143.9 (Ar), 130.1 (Ar), 125.8 (Ar), 124.4 (Ar), 123.6 (Ar), 122.6 (Ar), 118.6 (Ar), 114.3 (Ar), 114.0 (Ar), 100.1, 99.6 (2'-C, 4'-C), 74.3 (4-C), 68.2 (3-C), 63.7 (CH₂OH), 55.1 (2-C), 54.1 (6-C), 52.9 (CH₂-N), 50.4 (CH₂), 49.3 (CH₂), 48.2 (OCH₃), 48.0 (OCH₃), 40.9 (5-C), 31.9 (CH₂), 31.6 (CH₂), 30.3 (CH₂), 29.2 (CH₂), 28.9 (CH₂), 26.8 (CH₂), 26.5 (CH₂), 24.5 (CH₂), 22.8 (CH₂), 22.1 (CH₂), 18.1 (CH₃), 18.0 (CH₃). HRMS (ESI); calcd for C₃₆H₅₅N₆O₅⁺ 651.4228; found 651.4227.

General procedure for the preparation of compounds 12a–12d. A mixture of **24a**, **24b**, **24c** or **24d** (0.1 M) in 8 M aqueous HCl/MeOH (2:1) was stirred at room temperature for 24 hours. The volatiles were then removed under reduced pressure. The residue (0.25 M) was dissolved in 1 M aqueous NaOH/MeOH (29:160) and kept stirring for 4 hours at room temperature before the volatiles were removed under reduced pressure and the concentrate underwent purification by silica gel flash column chromatography.

N-((1-(2-((1,2,3,4-Tetrahydroacridin-9-yl)amino)ethyl)-1*H*-1,2,3-triazol-4-yl)methyl)isofagomine (**12a**). The crude product of **12a** was purified by silica gel column chromatography (CH₃CN/H₂O/NH₄OH 90:10:1) to provide **12a** (13.1 mg, 59%) as a yellow syrup. *R*_f 0.18 (CH₃CN/H₂O/NH₄OH 40:10:1); ¹H-NMR δ_H (CD₃OD, 400.13 MHz) 7.90–9.88 (1 H, m, ArH), 7.78 (1 H, dd, *J* = 0.7 Hz, *J* = 8.5 Hz, ArH), 7.69 (1 H, s, ArH), 7.61–7.57 (1 H, m, ArH), 7.41–7.37 (1 H, m, ArH), 4.63 (2 H, t, *J* = 5.6 Hz, CH₂), 4.08 (2 H, t, *J* = 5.6 Hz, CH₂), 3.73 (1 H, dd, *J*_{CHaOH;5} = 3.8 Hz, *J*_{CHaOH;CHbOH} = 10.9 Hz, CHaOH), 3.63–3.55 (2 H, m, CH₂-N), 3.46–3.40 (2 H, m, CHbOH, 3-H), 3.02–2.96 (3 H, m, 4-H, CH₂), 2.94–2.84 (2 H, m, 2a-H, 6a-H), 2.66 (2 H, t, *J* = 6.0 Hz, CH₂), 1.94–1.80 (6 H, m, 2b-H, 6b-H, 2 × CH₂), 1.72–1.63 (1 H, m, 5-H); ¹³C-NMR δ_C (CD₃OD, 100.61 MHz) 158.9 (Ar), 152.7 (Ar), 146.9 (Ar), 144.6 (Ar), 130.3 (Ar), 127.4 (Ar), 125.9 (Ar), 125.5 (Ar), 124.1 (Ar), 121.1 (Ar), 118.0 (Ar), 75.8 (4-C), 73.5 (3-C), 62.6 (CH₂OH), 59.1 (2-C), 56.0 (6-C), 53.2 (CH₂-N), 52.0 (CH₂), 48.9 (CH₂), 45.0 (5-C), 33.7 (CH₂), 26.0 (CH₂), 23.8 (CH₂), 23.4 (CH₂); HRMS (ESI); calcd for C₂₄H₃₃N₆O₃⁺ 453.2609; found 453.2602.

N-((1-(2-((1,2,3,4-Tetrahydroacridin-9-yl)amino)propyl)-1*H*-1,2,3-triazol-4-yl)methyl)isofagomine (**12b**). The crude product of **12b** was purified by silica gel column chromatography (CH₃CN/H₂O/NH₄OH 90:10:1 → 175:15:2) to provide **12b** (9.1 mg, 66%) as a colorless syrup. *R*_f 0.11 (CH₃CN/H₂O/NH₄OH 85:15:1); [α]_D²⁷ +10 (*c* 0.42, MeOH); ¹H-NMR δ_H (D₂O, 400.13 MHz) 2.67 (1 H, s, ArH), 7.49–7.44 (3 H, m, ArH), 7.17–7.13 (3 H, m, ArH), 4.37 (2 H, brs, CH₂), 3.67 (1 H, dd, *J*_{CHaOH;5} = 3.2 Hz, *J*_{CHaOH;CHaOH} = 11.5 Hz, CHaOH), 3.56 (2 H, s, CH₂-N), 3.53–3.47 (1 H, m, 3-H), 3.39 (1 H, dd, *J*_{CHbOH;5} = 7.0 Hz, *J*_{CHbOH;CHaOH} = 11.5 Hz, CHbOH), 3.34–3.32 (2 H, m, CH₂), 2.99–2.91 (2 H, 2a-H, 4-H), 2.85–2.82 (1 H, m, 6a-H), 2.67 (2 H, brs, CH₂), 2.22–2.15 (4 H, m, 2 × CH₂), 1.88–1.79 (4 H, m, 2b-H, 6b-H), 1.69 (5 H, brs, 5-H, 2 × CH₂); ¹³C-NMR δ_C (D₂O, 100.61 MHz) 155.5 (Ar), 152.2 (Ar), 142.8 (Ar), 141.8 (Ar), 130.2 (Ar), 125.2 (Ar), 124.2 (Ar), 123.7 (Ar), 123.1 (Ar), 117.6 (Ar), 114.7 (Ar), 73.6 (4-C), 71.2 (3-C), 60.7 (CH₂OH), 56.4 (2-C), 53.4 (6-C), 50.7 (CH₂-N), 48.0 (CH₂), 44.8 (CH₂), 42.8 (5-C), 31.0 (CH₂), 30.1 (CH₂), 23.9 (CH₂), 21.8 (CH₂), 21.2 (CH₂); HRMS (ESI); calcd for C₂₅H₃₅N₆O₃⁺ 467.2765; found 467.2760.

N-((1-(2-((1,2,3,4-Tetrahydroacridin-9-yl)amino)hexyl)-1*H*-1,2,3-triazol-4-yl)methyl)isofagomine (**12c**). The crude product of **12c** was purified by silica flash column chromatography (CH₃CN/H₂O/NH₄OH 185:15:1 → 180:20:1) to provide the title compound **12c** (30.5 mg, 73%) as a colorless wax. *R*_f 0.16 (CH₃CN/H₂O/NH₄OH 34:6:1); [α]_D²⁶ +15 (*c* 0.26, MeOH); ¹H-NMR δ_H (CD₃OD, 400.13 MHz) 8.13 (1 H, dd, *J* = 3.5 Hz, *J* = 8.5 Hz,

ArH), 7.85 (1 H, s, ArH), 7.79 (1 H, d, $J = 8.4$ Hz, ArH), 7.63–7.58 (1 H, m, ArH), 7.42–7.38 (1 H, m, ArH), 4.37–4.33 (2 H, m, CH₂), 3.79 (1 H, dd, $J_{\text{CHaOH};5} = 3.7$ Hz, $J_{\text{CHaOH};\text{CHbOH}} = 10.9$ Hz, CHaOH), 3.67 (2 H, s, CH₂-N), 3.62–3.57 (2 H, m, CH₂), 3.52–3.47 (2 H, m, CHbOH, 3-H), 3.05 (1 H, t, $J_{4;5} = 9.6$ Hz, 4-H), 3.01–2.98 (4 H, m, 2a-H, 6a-H, CH₂), 2.74–2.70 (2 H, m, CH₂), 1.95–1.04 (8 H, m, 2b-H, 6b-H, 3 × CH₂), 1.78–1.71 (1 H, m, 5-H), 1.69–1.62 (2 H, m, CH₂), 1.44–1.36 (2 H, m, CH₂), 1.33–1.28 (2 H, m, CH₂); ¹³C-NMR δ_C (CD₃OD, 100.61 MHz) 157.6 (Ar), 154.2 (Ar), 146.1 (Ar), 144.5 (Ar), 130.7 (Ar), 126.4 (Ar), 125.2 (Ar), 125.1 (Ar), 124.8 (Ar), 120.4 (Ar), 116.0 (Ar), 75.9 (4-C), 73.2 (3-C), 62.6 (CH₂OH), 59.2 (2-C), 56.0 (6-C), 53.3 (CH₂-N), 51.1 (CH₂), 49.3 (CH₂), 45.0 (5-C), 33.1 (CH₂), 31.9 (CH₂), 31.1 (CH₂), 27.2 (CH₂), 27.1 (CH₂), 25.9 (CH₂), 23.9 (CH₂), 23.3 (CH₂); HRMS (ESI); calcd for C₂₈H₄₁N₆O₃⁺ 509.3235; found 509.3228.

N-((1-(2-((1,2,3,4-Tetrahydroacridin-9-yl)amino)octyl)-1H-1,2,3-triazol-4-yl)methyl)isofagomine (12d). The crude product of **12d** was purified by silica flash column chromatography (CH₃CN/H₂O/NH₄OH 90 : 20 : 1) to provide the title compound **12d** (15.5 mg, 52%) as yellow syrup. R_f 0.14 (CH₃CN/H₂O/NH₄OH 170 : 30 : 3); $[\alpha]_D^{26} +15$ (c 0.55, MeOH); ¹H-NMR δ_H (CD₃OD, 400.13 MHz) 8.09 (1 H, dd, $J = 3.1$ Hz, $J = 8.5$ Hz, ArH), 7.87 (1 H, d, $J = 2.0$ Hz, ArH), 7.76 (1 H, d, $J = 8.5$ Hz, ArH), 7.57–7.53 (1 H, m, ArH), 7.38–7.34 (1 H, m, ArH), 4.36–4.32 (2 H, m, CH₂), 3.79 (1 H, dd, $J_{\text{CHaOH};5} = 3.7$ Hz, $J_{\text{CHaOH};\text{CHbOH}} = 10.9$ Hz, CHaOH), 3.68 (2 H, s, CH₂-N), 3.55–3.47 (4 H, m, CHbOH, 3-H, CH₂), 3.08–2.97 (5 H, m, 2a-H, 6a-H, 4-H, CH₂), 2.76–2.72 (2 H, m, CH₂), 1.95–1.89 (6 H, m, 2b-H, 6b-H, 2 × CH₂), 1.86–1.82 (2 H, m, CH₂), 1.78–1.70 (1 H, m, 5-H), 1.66–1.57 (2 H, m, CH₂), 1.34–1.31 (8 H, m, 4 × CH₂); ¹³C-NMR δ_C (CD₃OD, 100.61 MHz) 158.9 (Ar), 153.4 (Ar), 147.7 (Ar), 144.4 (Ar), 129.9 (Ar), 127.7 (Ar), 125.2 (Ar), 124.7 (Ar), 124.5 (Ar), 121.2 (Ar), 116.7 (Ar), 75.9 (4-C), 73.2 (3-C), 62.6 (CH₂OH), 59.2 (2-C), 56.0 (6-C), 53.3 (CH₂-N), 51.3 (CH₂), 49.3 (CH₂), 45.1 (5-C), 34.0 (CH₂), 32.2 (CH₂), 31.2 (CH₂), 30.1 (CH₂), 29.8 (CH₂), 27.7 (CH₂), 27.3 (CH₂), 26.1 (CH₂), 24.1 (CH₂), 23.7 (CH₂). HRMS (ESI); calcd for C₃₀H₄₅N₆O₃⁺ 537.3548; found 537.3542.

N-tert-Butoxycarbonyl-((2'S,3'S)-2',3',-dimethoxybutan-2',3'-diyl)isofagomine (25). **Step 1:** A degassed suspension of carbamate **21** (133 mg, 0.267 mmol, 1 equiv.) and Pd/C (10 wt%) in EtOH (14.4 mL) and AcOH (1.5 mL) was introduced an H₂-atmosphere (1 atm). The reaction mixture was kept stirring overnight at room temperature before the mixture was filtered through Celite and washed with CH₂Cl₂. The filtrate was concentrated under reduced. **Step 2:** The concentrate was dissolved in EtOH/H₂O (2 : 1; 3 mL) and was added NEt₃ (0.094 mL, 0.668 mmol, 2.5 equiv.) and Boc₂O (0.12 mL, 0.534 mmol, 2 equiv.). The mixture was kept stirring at room temperature overnight. The volatiles were then removed under reduced pressure and the concentrate underwent purification by silica gel flash column chromatography (EtOAc/PE 3 : 17 → 1 : 1) to provide the title compound **25** (47.8 g, 50%) as transparent syrup. R_f 0.47 (PE/EtOAc 1 : 1); $[\alpha]_D^{26} +158$ (c 0.43, MeOH); ¹H-NMR δ_H (CDCl₃, 400.13 MHz) 4.14 (2 H, brs, 2a-H,

6a-H), 3.74 (1 H, d, $J_{\text{CHaOH};5} = 6.1$ Hz, $J_{\text{CHaOH};\text{CHbOH}} = 10.9$ Hz, CHaOH), 3.67–3.58 (3 H, m, 3-H, 4-H, CHbOH), 3.27 (6 H, s, 2 × CH₃) 2.65 (1 H, brs, 2b-H), 2.53–2.47 (1 H, m, 6b-H), 2.04–1.85 (2 H, m, OH, 5-H), 1.44 (9 H, s, C(CH₃)₃), 1.31 (3 H, s, CH₃), 1.30 (3 H, s, CH₃); ¹³C-NMR δ_C (CDCl₃, 100.61 MHz) 154.8 (C=O), 100.1, 99.7 (2'-C, 3'-C), 80.4 (C(CH₃)₃), 73.8, 67.6 (3-C, 4-C), 62.8 (CH₂OH), 48.2, 48.1 (OCH₃), 46.4, 45.4 (2-C, 6-C), 41.2 (5-C), 28.5 (C(CH₃)₃), 18.0, 17.8 (CH₃); HRMS (ESI); calcd for C₁₇H₃₁NO₇Na⁺ 384.1993; found 384.1990.

Isifagomine hydrochloride (6HCl). A mixture of **25** (50 mg, 0.138 mmol) in 8 M aqueous HCl (10 mL) and MeOH (4.5 mL) was stirred overnight at room temperature. The volatiles were then removed under reduced pressure. The concentrate was dissolved 0.6 M aqueous HCl (20 mL) and washed with CHCl₃ (2 × 20 mL). The aqueous layer was concentrated under reduced pressure to provide the title compound **6HCl** (18.4 mg, 73%) as a light-yellow syrup. The NMR data was in agreement with reported data;⁵⁵ ¹H-NMR δ_H (D₂O, 400.13 MHz) 3.83 (1 H, dd, $J = 3.2$, $J = 11.3$), 3.80–3.73 (2 H, m), 3.55–3.50 (3 H, m), 3.01–2.94 (1 H, m), 2.91–2.85 (1 H, m), 2.00–1.93 (1 H, m); ¹³C-NMR δ_C (D₂O, 100.61 MHz) 71.1, 68.5, 59.0, 46.6, 44.8, 41.0.

General procedure for preparation of compounds 27a–27c. A mixture of alkyne **26** (0.07 M, 1 equiv.), azide **23**, **17** or **18** (0.07 M, 1 equiv.), and copper(II) sulfate pentahydrate (0.30 equiv.) in DMF in a foil covered round bottom flask was degassed and introduced a N₂-atmosphere before the addition of sodium ascorbate (0.60 equiv.). After addition, the mixture was kept stirring overnight at room temperature. After this time, the solvent was removed under reduced pressure and the residue was purified by silica gel column chromatography.

N-((1-(2-((1,2,3,4-Tetrahydroacridin-9-yl)amino)ethyl)-1H-1,2,3-triazol-4-yl)methyl)-2,3,4,6-tetra-O-benzyl-1-deoxynojirimycin (27a). The crude product of **27a** was purified by silica gel flash column chromatography (CH₂Cl₂/MeOH 9 : 1 → 17 : 3) to obtain the title compound **27a** (66 mg, 94%) as a yellow syrup. R_f 0.43 (CH₂Cl₂/MeOH 9 : 1); $[\alpha]_D^{26} +6$ (c 0.66, EtOAc); ¹H-NMR δ_H (CDCl₃, 400.13 MHz) 7.93 (1 H, d, $J = 8.3$ Hz, ArH), 7.76 (1 H, d, $J = 8.4$ Hz, ArH), 7.51 (1 H, t, $J = 7.3$ Hz, ArH), 7.35–7.19 (20 H, m, ArH), 7.08–7.07 (2 H, m, ArH), 4.89 (1 H, d, $J = 11.0$ Hz, CHPh), 4.83 (1 H, d, $J = 10.8$ Hz, CHPh), 4.73 (1 H, d, $J = 11.0$ Hz, CHPh), 4.51 (2 H, s, 2 × CHPh), 4.51 (1 H, d, $J = 11.9$ Hz, CHPh), 4.46–4.42 (3 H, m, CHPh, CH₂), 4.33 (1 H, d, $J = 10.8$ Hz, CHPh), 4.17 (1 H, d, $J_{\text{CHaN};\text{CHbN}} = 15.3$ Hz, CHaN), 3.94–3.92 (3 H, m, 6a-H, CH₂), 3.90–3.89 (1 H, m, CHbN), 3.71 (1 H, dd, $J_{6b;5} = 2.3$ Hz, $J_{6a;6b} = 10.5$ Hz, 6b-H), 3.64 (1 H, ddd, $J_{2;1a} = 4.8$ Hz, $J_{2;3} = 9.2$ Hz, $J_{2;1b} = 10.2$ Hz, 2-H), 3.50 (1 H, t, $J_{4;5} = 9.3$ Hz, 4-H), 3.31 (1 H, t, $J_{3;2} = 9.2$ Hz, 3-H), 3.12 (1 H, dd, $J_{1a;2} = 4.8$ Hz, $J_{1a;1b} = 11.2$ Hz, 1a-H), 3.06–3.03 (2 H, m, CH₂), 2.61–2.59 (2 H, m, CH₂), 2.22 (1 H, dt, $J_{5;6} = 2.3$ Hz, $J_{5;4} = 9.3$ Hz, 5-H), 2.16–2.10 (1 H, m, 1b-H), 1.84–1.83 (4 H, m, 2 × CH₂); ¹³C-NMR δ_C (CDCl₃, 100.61 MHz) 158.1 (Ar), 150.0 (Ar), 146.2 (Ar), 142.5 (Ar), 138.9 (Ar), 138.5 (Ar), 137.8 (Ar), 129.1–127.6 (Ar), 124.7 (Ar), 124.1 (Ar), 122.3 (Ar), 120.2 (Ar), 117.5 (Ar), 87.0 (3-C), 78.6 (4-C), 78.3 (2-C), 75.4 (CH₂Ph), 75.3 (CH₂Ph), 73.6 (CH₂Ph), 72.7 (CH₂Ph), 66.6 (6-C), 62.8 (5-C),

54.7 (1-C), 50.6 (CH₂), 47.9 (CH₂), 47.3 (CH₂-N), 33.3 (CH₂), 24.9 (CH₂), 22.9 (CH₂), 22.5 (CH₂); HRMS (ESI); calcd for C₅₂H₅₇N₆O₄⁺ 829.4436; found 829.4432.

***N*-((1-(2-((1,2,3,4-Tetrahydroacridin-9-yl)amino)propyl)-1*H*-1,2,3-triazol-4-yl)methyl)-2,3,4,6-tetra-*O*-benzyl-1-deoxynojirimycin (27b).**

The crude product of 27b was purified by silica gel column chromatography (CH₂Cl₂/MeOH 19.1 → 9 : 1) to obtain the title compound 27b (32 mg, 50%) as a light yellow syrup. *R*_f 0.23 (CH₂Cl₂/MeOH 9 : 1); [α]_D²⁷ +12 (c 0.33, CH₂Cl₂); ¹H-NMR δ_H (CDCl₃, 400.13 MHz) 7.99 (1 H, d, *J* = 8.5 Hz, ArH), 7.60–7.56 (1 H, m, ArH), 7.41–7.34 (4 H, m, ArH), 7.31–7.23 (17 H, m, ArH), 7.11–7.08 (2 H, m, ArH), 4.90 (1 H, d, *J* = 11.0 Hz, CHPh), 4.86 (1 H, d, *J* = 10.7 Hz, CHPh), 4.75 (1 H, d, *J* = 11.0 Hz, CHPh), 4.64 (2 H, s, 2 × CHPh), 4.56 (1 H, d, *J* = 11.9 Hz, CHPh), 4.47 (1 H, d, *J* = 11.9 Hz, CHPh), 4.43 (2 H, t, *J* = 6.4 Hz, CH₂), 4.36 (1 H, d, *J* = 10.7 Hz, CHPh), 4.21 (1 H, d, *J*_{CHaN;CHbN} = 15.3 Hz, CHaN), 3.98–3.93 (2 H, m, 6a-H, CHbN), 3.74 (1 H, dd, *J*_{6b;5} = 2.9 Hz, *J*_{6a;6b} = 10.5 Hz, 6b-H), 3.69–3.63 (3 H, m, CH₂, 2-H), 3.53 (1 H, t, *J*_{4;5} = 9.3 Hz, 4-H), 3.32 (1 H, t, *J*_{3;2} = 9.1 Hz, 3-H), 3.18–3.12 (3 H, m, CH₂, 1a-H), 2.69–2.68 (2 H, m, CH₂), 2.27–2.24 (3 H, m, CH₂, 5-H), 2.22 (1 H, t, *J*_{1b;1a} = 11.2 Hz, 1b-H), 1.89–1.88 (4 H, m, 2 × CH₂); ¹³C-NMR δ_C (CDCl₃, 100.61 MHz) 142.6 (Ar), 138.9 (Ar), 138.5 (Ar), 138.4 (Ar), 137.9 (Ar), 128.6–127.7 (Ar), 125.0 (Ar), 123.6 (Ar), 122.9 (Ar), 87.1 (3-C), 78.6 (4-C), 78.4 (2-C), 75.5 (CH₂Ph), 75.4 (CH₂Ph), 73.7 (CH₂Ph), 72.8 (CH₂Ph), 66.7 (6-C), 62.8 (5-C), 54.7 (1-C), 47.5 (CH₂), 47.4 (CH₂-N), 45.2 (CH₂), 31.2 (CH₂), 29.8 (CH₂), 24.7 (CH₂), 22.6 (CH₂), 21.9 (CH₂). HRMS (ESI); calcd for C₅₃H₅₈N₆O₄Na⁺ 865.4412; found 865.4396.

***N*-((1-(2-((1,2,3,4-Tetrahydroacridin-9-yl)amino)hexyl)-1*H*-1,2,3-triazol-4-yl)methyl)-2,3,4,6-tetra-*O*-benzyl-1-deoxynojirimycin (27c).**

The crude product of 27c was purified by silica gel column chromatography (CH₂Cl₂/MeOH 49 : 1 → 47 : 8) to obtain the title compound 27c (42 mg, 48%) as a light-yellow syrup. *R*_f 0.73 (CH₂Cl₂/EtOH/NH₄OH 90 : 10 : 1); [α]_D²⁷ +7 (c 0.29, CH₂Cl₂); ¹H-NMR δ_H (CDCl₃, 400.13 MHz) 8.40 (1 H, d, *J* = 8.3 Hz, ArH), 8.13 (1 H, d, *J* = 8.6 Hz, ArH), 7.61 (1 H, t, *J* = 7.6 Hz, ArH), 7.38 (1 H, t, *J* = 7.6 Hz, ArH), 7.33–7.21 (19 H, m, ArH), 7.07–7.04 (2 H, m, ArH), 4.88 (1 H, d, *J* = 11.0 Hz, CHPh), 4.82 (1 H, d, *J* = 10.7 Hz, CHPh), 4.73 (1 H, d, *J* = 11.0 Hz, CHPh), 4.61 (2 H, s, 2 × CHPh), 4.56 (1 H, d, *J* = 12.0 Hz, CHPh), 4.45 (1 H, d, *J* = 11.9 Hz, CHPh), 4.32 (1 H, d, *J* = 10.7 Hz, CHPh), 4.26 (2 H, t, *J* = 7.0 Hz, CH₂), 4.18 (1 H, d, *J*_{CHaN;CHbN} = 15.2 Hz, CHaN), 3.97–3.94 (1 H, m, 6a-H), 3.92 (1 H, d, *J*_{CHbN;CHaN} = 15.2 Hz, CHbN), 3.83 (2 H, t, *J* = 7.0 Hz, CH₂), 3.72 (1 H, dd, *J*_{6b;5} = 2.5 Hz, *J*_{6b;6a} = 10.5 Hz, 6b-H), 3.68–3.62 (1 H, m, 2-H), 3.53 (1 H, t, *J*_{4;5} = 9.3 Hz, 4-H), 3.32 (1 H, t, *J*_{3;2} = 9.1 Hz, 3-H), 3.22 (2 H, t, *J* = 5.6 Hz, CH₂), 3.12 (1 H, dd, *J*_{1a;2} = 4.8 Hz, *J*_{1a;1b} = 11.0 Hz, 1a-H), 2.59 (2 H, t, *J* = 5.8 Hz, CH₂), 2.22 (1 H, dt, *J*_{5;6} = 2.5 Hz, *J*_{5;4} = 9.3 Hz, 5-H), 2.13 (1 H, t, *J*_{1b;1a} = 11.0 Hz, 1b-H), 1.89–1.75 (8 H, m, 4 × CH₂), 1.50–1.43 (2 H, m, CH₂), 1.37–1.30 (2 H, m, CH₂). ¹³C-NMR δ_C (CDCl₃, 100.61 MHz) 154.9 (Ar), 152.4 (Ar), 142.0 (Ar), 140.0 (Ar), 138.9 (Ar), 138.5 (Ar), 138.4 (Ar), 137.9 (Ar), 131.9 (Ar), 128.5–127.6 (Ar), 125.1 (Ar), 124.1 (Ar), 123.0 (Ar), 122.0 (Ar), 116.5 (Ar), 111.6 (Ar), 87.2 (3-C), 78.6 (2-C), 78.4 (4-C), 75.5 (CH₂Ph), 75.4 (CH₂Ph), 73.3

(CH₂Ph), 72.8 (CH₂Ph), 66.4 (6-C), 62.8 (5-C), 54.6 (1-C), 49.9 (CH₂), 48.4 (CH₂), 47.4 (CH₂-N), 31.0 (CH₂), 30.0 (CH₂), 29.2 (CH₂), 26.0 (CH₂), 25.9 (CH₂), 24.0 (CH₂), 22.1 (CH₂), 21.0 (CH₂); HRMS (ESI); calcd for C₅₆H₆₅N₆O₄⁺ 885.5055; found 885.5062.

General procedure for the preparation of compounds 13a–13c. A solution of compound 27a, 27b or 27c (0.045 M) in anhydrous CH₂Cl₂ under a N₂-atmosphere at –78 °C was slowly added BCl₃ (1 M in heptane, 20 equiv.). After addition, the mixture was kept stirring at –78 °C for 2 hours and then at 0 °C overnight. The mixture was added aqueous NaOH (1 M, 60 equiv.)/CH₃OH (13 : 15) and was kept stirring at 0 °C for 10 minutes. After this time, the volatiles were removed under reduced pressure and the concentrate underwent purification by silica gel column chromatography.

***N*-((1-(2-((1,2,3,4-Tetrahydroacridin-9-yl)amino)ethyl)-1*H*-1,2,3-triazol-4-yl)methyl)-1-deoxynojirimycin (13a).**

The crude product of 13a was purified by silica column chromatography (MeCN/H₂O/NH₄OH 950 : 50 : 1 → 850 : 150 : 1) to provide the title compound 13a (20 mg, 64%) as a yellow syrup. *R*_f 0.11 (MeCN/H₂O 17 : 3); [α]_D²⁷ –4 (c 0.51, MeOH/H₂O 8 : 1); ¹H-NMR δ_H (D₂O, 400.13 MHz) 7.82 (1 H, d, *J* = 8.6 Hz, ArH), 7.76 (1 H, t, *J* = 7.4 Hz, ArH), 7.68 (1 H, s, ArH), 7.56 (1 H, d, *J* = 7.4 Hz, ArH), 7.50–7.46 (1 H, m, ArH), 4.70–4.67 (2 H, m, CH₂), 4.38–4.36 (2 H, m, CH₂), 3.85 (1 H, dd, *J*_{6a;5} = 2.2 Hz, *J*_{6a;6b} = 12.8 Hz, 6a-H), 3.77 (1 H, d, *J*_{CHaN;CHbN} = 15.3 Hz, CHaN), 3.72 (1 H, dd, *J*_{6b;5} = 2.2 Hz, *J*_{6b;6a} = 12.8 Hz, 6b-H), 3.60 (1 H, d, *J*_{CHbN;CHaN} = 15.3 Hz, CHbN), 3.41 (1 H, ddd, *J*_{2;1a} = 4.9 Hz, *J*_{2;3} = 9.2 Hz, *J*_{2;1b} = 10.5 Hz, 2-H), 3.30 (1 H, t, *J*_{4;5} = 9.4 Hz, 4-H), 2.86 (2 H, brs, CH₂), 2.79 (1 H, t, *J*_{3;2} = 9.2 Hz, 3-H), 2.72 (1 H, dd, *J*_{1a;2} = 4.9 Hz, *J*_{1a;1b} = 11.1 Hz, 1a-H), 2.45 (2 H, brs, CH₂), 1.86–1.85 (4 H, m, 2 × CH₂), 1.68 (1 H, t, *J*_{1b;1a} = 11.1 Hz, 1b-H), 1.56 (1 H, dt, *J*_{5;6} = 2.2 Hz, *J*_{5;4} = 9.4 Hz, 5-H); ¹³C-NMR δ_C (D₂O, 100.61 MHz) 156.1 (Ar), 151.7 (Ar), 140.8 (Ar), 137.6 (Ar), 132.7 (Ar), 125.5 (Ar), 125.4 (Ar), 123.8 (Ar), 119.4 (Ar), 115.4 (Ar), 113.4 (Ar), 78.0 (3-C), 69.4 (4-C), 68.5 (2-C), 63.5 (5-C), 56.8 (6-C), 55.3 (1-C), 51.0 (CH₂), 47.0 (CH₂), 45.4 (CH₂-N), 28.2 (CH₂), 23.5 (CH₂), 21.2 (CH₂), 20.2 (CH₂); HRMS (ESI); calcd for C₂₄H₃₃N₆O₄⁺ 469.2558; found 469.2560.

***N*-((1-(2-((1,2,3,4-Tetrahydroacridin-9-yl)amino)propyl)-1*H*-1,2,3-triazol-4-yl)methyl)-1-deoxynojirimycin (13b).**

The crude product of 13b was purified by silica gel column chromatography (CH₃CN/H₂O/NH₄OH 90 : 10 : 1 → 85 : 15 : 1) to provide the title compound 13b (18 mg, 90%) as a yellow syrup. *R*_f 0.11 (CH₃CN/H₂O/NH₄OH 190 : 50 : 1); ¹H-NMR δ_H (D₂O, 400.13 MHz) 7.85 (1 H, s, ArH), 7.72–7.69 (2 H, m, ArH), 7.48 (1 H, d, *J* = 8.7 Hz, ArH), 7.34 (1 H, t, *J* = 7.8 Hz, ArH), 4.51 (2 H, t, *J* = 5.9 Hz, CH₂), 3.99 (1 H, dd, *J*_{6a;5} = 2.4 Hz, *J*_{6a;6b} = 12.7 Hz, 6a-H), 3.89–3.85 (2 H, m, CHaN, 6b-H), 3.81–3.77 (3 H, m, CHbN, CH₂), 3.53–3.47 (1 H, m, 2-H), 3.40 (1 H, t, *J*_{4;5} = 9.4 Hz, 4-H), 3.01 (1 H, t, *J*_{3;2} = 9.3 Hz, 3-H), 2.88 (1 H, dd, *J*_{1a;2} = 4.9 Hz, *J*_{1a;1b} = 11.2 Hz, 1a-H), 2.80 (2 H, brs, CH₂), 2.39–2.32 (4 H, m, 2 × CH₂), 2.05–1.97 (2 H, m, 5-H, 1b-H), 1.83 (4 H, brs, 2 × CH₂); ¹³C-NMR δ_C (D₂O, 100.61 MHz) 155.5 (Ar), 150.1 (Ar), 140.5 (Ar), 137.2 (Ar), 132.8 (Ar), 125.5 (Ar), 124.9 (Ar), 124.2 (Ar), 118.5 (Ar), 114.5 (Ar), 111.4 (Ar), 77.8 (3-C), 69.4 (4-C),

68.4 (2-C), 64.0 (5-C), 56.8 (6-C), 55.1 (1-C), 48.0 (CH₂), 45.7 (CH₂-N), 44.6 (CH₂), 29.3 (CH₂), 27.8 (CH₂), 23.2 (CH₂), 21.2 (CH₂), 20.1 (CH₂). HRMS (ESI); calcd for C₂₂H₃₅N₆O₄⁺ 483.2714; found 483.2702.

N-((1-(2-((1,2,3,4-Tetrahydroacridin-9-yl)amino)hexyl)-1*H*-1,2,3-triazol-4-yl)methyl)-1-deoxynojirimycin (**13c**). The crude product of **13c** was purified by silica gel column chromatography (MeCN/H₂O/NH₄OH 975:25:1 → 850:150:1) to provide the title compound **13c** (24 mg, 97%) as a yellow solid. *R*_f 0.13 (CH₃CN/H₂O/NH₄OH 850:150:1); [α]_D²⁶ -8 (*c* 0.23, MeOH/H₂O 2:1); ¹H-NMR δ _H (D₂O, 400.13 MHz) 7.92 (1 H, s, ArH), 7.83 (1 H, d, *J* = 8.7 Hz, ArH), 7.63 (1 H, t, *J* = 7.7 Hz, ArH), 7.41 (1 H, d, *J* = 8.4 Hz, ArH), 7.30 (1 H, t, *J* = 7.7 Hz, ArH), 4.34 (2 H, t, *J* = 6.7 Hz, CH₂), 4.07 (1 H, dd, *J*_{6a;5} = 1.9 Hz, *J*_{6a;6b} = 12.8 Hz, 6a-H), 3.96–3.85 (3 H, m, CH₂-N, 6b-H), 3.57–3.54 (2 H, m, CH₂), 3.50 (1 H, dd, *J*_{2;1a} = 4.8 Hz, *J*_{2;1b} = 10.1 Hz, 2-H), 3.41 (1 H, t, *J*_{4;5} = 9.5 Hz, 4-H), 3.07 (1 H, t, *J*_{3;2} = 9.2 Hz, 3-H), 2.92 (1 H, dd, *J*_{1a;2} = 4.8 Hz, *J*_{1a;1b} = 11.2 Hz, 1a-H), 2.74 (2 H, brs, CH₂), 2.31 (2 H, brs, CH₂), 2.07 (1 H, t, *J*_{1b;1a} = 11.2 Hz, 1b-H), 2.01–1.98 (1 H, m, 5-H), 1.86–1.79 (6 H, m, 3 × CH₂), 1.59 (2 H, q, *J* = 7.1 Hz, CH₂), 1.29 (2 H, q, *J* = 7.3 Hz, CH₂), 1.20–1.13 (2 H, m, CH₂). ¹³C-NMR δ _H (D₂O, 100.61 MHz) 155.2 (Ar), 150.3 (Ar), 140.9 (Ar), 138.1 (Ar), 132.3 (Ar), 125.3 (Ar), 124.6 (Ar), 119.1 (Ar), 114.9 (Ar), 111.4 (Ar), 78.1 (3-C), 69.7 (4-C), 68.6 (2-C), 64.1 (5-C), 57.0 (6-C), 55.4 (1-C), 50.1 (CH₂), 47.3 (CH₂), 45.9 (CH₂-N), 29.4 (CH₂), 29.1 (CH₂), 28.1 (CH₂), 25.1 (CH₂), 25.0 (CH₂), 23.0 (CH₂), 21.3 (CH₂), 20.2 (CH₂); HRMS (ESI); calcd for C₂₈H₄₁N₆O₄⁺ 525.3184; found 525.3179.

Inhibition assays

For measuring the anti-cholinesterase activity of title compounds, a double-beam Hitachi U-2900 spectrophotometer was used, following the classical Ellman's assay, with minor modifications.⁵⁶

In PS cuvettes (1.2 mL final volume), the following concentrations were fixed: 0.975 mM 5,5'-dithiobis(2-nitrobenzoic acid) (DTNB), 50 μ M phosphate buffer (pH 8.0); 5 different substrate concentrations were used, ranging from 0.25 to 4.0 of the expected *K*_M value. Two different sets of experiments were performed: one without inhibitor, and another one with 3,4 different inhibitor concentrations (giving roughly 30–80% inhibition at [*S*] = *K*_M). The enzyme was appropriately diluted so as to give a reaction rate within 0.12–0.15 Abs min⁻¹ at the highest substrate concentration in the absence of inhibitor. Reaction was monitored at 405 nm during 125 s, *T* = 25 °C.

The mode of inhibition was doubly determined using the CornishBowden (1/*v* vs. [*I*], [*S*]/*v* vs. [*I*]) plots.⁵⁷

Kinetic parameters (*K*_M, *V*_{max}) were obtained using non-linear regression analysis (least squares fit) using GraphPad Prism 8.01 software; inhibition constants were calculated using the following equations:

Competitive inhibition:

$$K_{ia} = \frac{[I]}{\frac{K_{M \text{ app}}}{K_M} - 1}$$

Mixed inhibition:

$$K_{M \text{ app}} = K_M \frac{1 + \frac{[I]}{K_{ia}}}{1 + \frac{[I]}{K_{ib}}}$$

$$V_{\text{max app}} = \frac{V_{\text{max}}}{1 + \frac{[I]}{K_{ib}}}$$

Non-competitive:

$$K_{M \text{ app}} = K_M$$

$$V_{\text{max app}} = \frac{V_{\text{max}}}{1 + \frac{[I]}{K_i}}$$

Modelling and simulation methods

Protein model. The protein model is a monomer based on the crystal structure of acetylcholinesterase from *Electrophorus Electricus* (pdb code 1C2B).⁵⁸ Missing atoms (side chains of Asp491, Arg492, Asp494, Ser495, Lys 496, and Ser497 as well as hydrogen atoms) have been added using the coordinates estimated by the psfgen plugin of the VMD software suite.⁵⁹

Ligand models

As ligands, we have modelled compounds **12a**, **12c** and compounds **13a** and **13c**, representing the ligands with the shortest (*n* = 2) and the longest linkers (*n* = 5) available with both iminosugar variants. Since the p*K*_a values of the isolated iminosugars as well as that of tacrine (p*K*_a = 9.8)⁶⁰ suggest these moieties to be protonated, we have set up models in which each of the ligands is protonated either at the nitrogen atom of the iminosugar moiety (sugNH) or the nitrogen atom of the tacrine ring system (tacNH). Note that in contrast to earlier modelling studies of bis-tacrine⁶¹ in which both tacrine moieties were protonated, we decided to model the ligand with a single positive charge, *i.e.* one site protonated.

These models have been optimised on the Hartree-Fock level of theory with a 6-31G(d) basis set and using the Gaussian programme.⁶² On the optimized geometries, electrostatic potentials have been calculated so as to obtain RESP charges and GAFF parameters⁶³ for the ligands therefrom. Those force field parameters were determined employing antechamber.⁶⁴

Protein-ligand complexes

The AChE receptor protein from another organism, *Torpedo californica*, that has a ligand, similar to our AChEIs, bound,²⁹ shows a slightly different active site conformation than the 1c2b structure from *Electrophorus Electricus* (see supporting Fig. S1†). In particular, the conformation of residue Tyr337 in *Electrophorus Electricus* is unfavorable for ligand binding compared to the conformation of the corresponding Phe330 in *Torpedo californica*. We have therefore altered the confor-

1 matation of residue Tyr337 such that it coincides with the con- 1
formation of Phe330.

Models of protein–ligand complexes have been built by 5
docking the ligand molecules into the AChE receptor protein
with altered Y337 conformation using vina autodock⁶⁵ with all
non-cyclic single bonds treated as rotatable. The search space
was $22 \times 24 \times 24 \text{ \AA}^3$. Up to 9 poses within a maximum of 3 kcal
mol⁻¹ difference in estimated binding affinity were generated
for each ligand and starting conformation. From the thus gener- 10
ated poses, two for each model were selected for subsequent
MD simulations comprising pose 1, with the tacrine at the CAS
inside the protein (and the iminosugar moiety towards the PAS
at the mouth of the protein) and pose 2 with the iminosugar
moiety at the CAS inside the protein (and the tacrine moiety at 15
the PAS). For ligand **12a**, in both protonation states, sugH and
tacH, no pose 1 could be obtained by the automated docking,
rather these models were generated by manually docking the
ligand into the protein, using a pose obtained from docking to 20
the AChE receptor protein from *Torpedo californica* (1ut6) as a
template.

The total set of model complexes thus generated is:

12a sugNH	12c sugNH	13a sugNH	13c sugNH
pose 1	pose 1	pose 1	pose 1
12a sugNH	12c sugNH	13a sugNH	13c sugNH
pose 2	pose 2	pose 2	pose 2
12a tacNH pose	12c tacNH pose	13a tacNH pose	13c tacNH pose
1	1	1	1
12a tacNH pose	12c tacNH pose	13a tacNH pose	13c tacNH pose
2	2	2	2

MD simulations. Molecular dynamics simulations were 30
carried out using the Amber14SB force field⁶⁶ for the protein
and GAFF parameters (see above) for ligands. The systems were
solvated in a cubic box of 11 nm. The boxes were filled with
TIP3P water,⁶⁷ sodium and chloride ions added for neutralisa- 35
tion, and an additional salt concentration of 150 mmol L⁻¹ so
as to mimic physiological conditions. The temperature was con-
trolled to be at 300 K employing the V-rescale thermostat.⁶⁸ After
200 ps equilibration with the solute atoms constrained, 200 ns
production run was performed for each system. Only the last 100
ns of each of the simulations was used for analysis so as to allow
sufficient equilibration time for the ligand and protein and
thereby reduce bias from the initial structure preparation. For 40
MD simulations and analysis, the gromacs programme, version
2019.6⁶⁹ was employed. Molecule figures were generated using
VMD and python molecule viewer.⁷⁰

Author contributions

Conceptualization, E.L. and Ó.L.; methodology, E.L., Ó.L., P.I., 55
Q.L.O.S., and T.C.S.E.; formal analysis, P.I.; funding acqui-
sition, M.O.S. and S.B.F.; investigation, E.L., Ó.L., P.I., Q.L.O.
S., and T.C.S.E.; project administration, E.L., Ó.L., and P.I.;
resources, E.L., Ó.L., P.I., M.O.S., and J.G.F.B.; supervision, E.L.
and M.O.S.; writing – original draft, E.L., Ó.L., P.I., Q.L.O.S.,

and T.C.S.E.; writing – review & editing, E.L., Ó.L., P.I., Q.L.O.S., 1
T.C.S.E., M.O.S., and J.G.F.B.

Conflicts of interest

 5

There are no conflicts to declare.

Acknowledgements

 10

Q. L. O. S. is grateful for the provision of a three-month scho- 15
larship from the Diku funded NorBra project enabling a
research stay at the University of Stavanger; T. C. S. E would
like to thank Coordenação de Aperfeiçoamento de Pessoal de
Nível Superior – Brasil (CAPES) for a PhD fellowship. We thank
Associate Professor Kåre B. Jørgensen for keeping the NMR
instrument in good condition. We also thank the Dirección
General de Investigación of Spain (CTQ2016-78703-P), the 20
Junta de Andalucía (FQM134), the European Regional
Development Fund (FEDER) for financial support.

Notes and references

 25

- 1 H. W. Querfurth and F. M. LaFerla, *N. Engl. J. Med.*, 2010, 362, 329.
- 2 (a) L. Pini, M. Pievania, M. Bocchetta, D. Altomarea, P. Boscoa, E. Cavedoa, S. Galluzzia, M. Marizzonia and G. B. Frisoni, *Ageing Res. Rev.*, 2016, 30, 25; (b) T. H. Ferreira-Vieira, I. M. Guimaraes, F. R. Silva and F. M. Ribeiro, *Curr. Neuropharmacol.*, 2016, 14, 101.
- 3 M. G. Savelieff, G. Nam, J. Kang, H. J. Lee, M. Lee and M. H. Lim, *Chem. Rev.*, 2019, 119, 1221.
- 4 G. S. Bloom, *JAMA Neurol.*, 2014, 71, 505–508.
- 5 M. T. Heneka, M. K. O'Banion, D. Terwel and D. M. P. Kummer, *J. Neural Transm.*, 2010, 117, 919.
- 6 C. J. Ledner and J. M. Lee, *J. Neuropathol. Exp. Neurol.*, 1998, 57, 719.
- 7 M. A. Greenough, J. Camakaris and A. I. Bush, *Neurochem. Int.*, 2013, 62, 540.
- 8 P. Zatta, D. Drago, S. Bolognin and S. L. Sensi, *Trends Pharmacol. Sci.*, 2009, 7, 346.
- 9 Alzheimer's Association (2016), *Alzheimers Dement*, 2016, 12, 459.
- 10 L. A. Craig, N. S. Hong and R. J. McDonald, *Neurosci. Biobehav. Rev.*, 2011, 35, 1397.
- 11 Y.-H. Lou, J.-S. Wang, G. Dong, P.-P. Guo, D.-D. Wei, S.-S. Xie, M.-H. Yang and L.-Y. Kong, *Toxicol. Res.*, 2015, 4, 1465.
- 12 <https://www.alz.org/media/documents/fda-approved-treatments-alzheimers-ts.pdf>, accessed December 7, 2020.
- 13 N. Tabet, *Age Ageing*, 2006, 35, 336.
- 14 (a) R. T. Bartus, *Exp. Neurol.*, 2000, 163, 495; (b) R. T. Bartus, R. L. Dean, 3rd, B. Beer and A. S. Lippa, *Science*, 1982, 217, 408.

- 1 15 R. Cimler, P. Maresova, J. Kuhnova and K. Kuca, *PLoS One*, 2019, **14**, e0210958.
- 16 H. Soreq and H. Zakut, *Human Cholinesterases and Anticholinesterases*, Academic Press, New York, 1993.
- 5 17 N. H. Greig, T. Utsuki, Q. Yu, X. Zhu, H. W. Holloway, T. Perry, B. Lee, D. K. Ingram and D. K. Lahiri, *Curr. Med. Res. Opin.*, 2001, **17**, 159.
- 18 Q. Li, H. Yang, Y. Chen and H. Sun, *Eur. J. Med. Chem.*, 2017, **132**, 294.
- 10 19 M. Weinstock, *CNS Drugs*, 1999, **12**, 307.
- 20 20 S. Gupta and C. G. Mohan, *BioMed. Res. Int.*, 2014, 291214.
- 21 P. Anand and B. Singh, *Bioorg. Med. Chem.*, 2012, **20**, 521.
- 22 J. L. Sussman, M. Harel, F. Frolow, C. Oefner, A. Goldman, L. Toker and I. Silman, *Science*, 1991, **253**, 872.
- 15 23 (a) N. C. Inestrosa, A. Alvarez, C. A. Pérez, R. D. Moreno, M. Vicente, C. Linker, O. I. Casanueva, C. Soto and J. Garrido, *Neuron*, 1996, **16**, 881; (b) G. V. De Ferrari, M. A. Canales, I. Shin, L. M. Weiner, I. Silman and N. C. Inestrosa, *Biochemistry*, 2001, **40**, 10447.
- 20 24 M. Bartolini, C. Bertucci, V. Cavrini and V. Andrisano, *Biochem. Pharmacol.*, 2003, **65**, 407.
- 25 25 (a) L. Piazzzi, A. Rampa, A. Bisi, S. Gobbi, F. Belluti, A. Cavalli, M. Bartolini, V. Andrisano, P. Valenti and M. Recanatini, *J. Med. Chem.*, 2003, **46**, 2279–2282; (b) H. Tang, L.-Z. Zhao, H.-T. Zhao, S.-L. Huang, S.-M. Zhong, J.-K. Qin, Z.-F. Chen, Z.-S. Huang and H. Liang, *Eur. J. Med. Chem.*, 2011, **46**, 4970; (c) A. Minarini, A. Milelli, V. Tumiatti, M. Rosini, E. Simoni, M. L. Bolognesi, V. Andrisano, M. Bartolini, E. Motori, C. Angeloni and S. Hrelia, *Neuropharmacology*, 2012, **62**, 997; (d) V. K. Meena, S. Chaturvedi, R. K. Sharma, A. K. Mishra and P. P. Hazari, *Mol. Pharm.*, 2019, **16**, 2296.
- 30 26 (a) I. Zueva, J. Dias, S. Lushchekina, V. Semenov, M. Mukhamedyarov, T. Pashirova, V. Babaev, F. Nachon, N. Petrova, L. Nurullin, L. Zakharova, V. Ilyin, P. Masson and K. Petrov, *Neuropharmacology*, 2019, **155**, 131; (b) T. Silva, J. Reis, J. Teixeira and F. Borges, *Ageing Res. Rev.*, 2014, **15**, 116.
- 35 27 J. L. Sussman, I. Silman, P. H. Axelsen, C. Hirth, M. Goeldner, F. Bouet, L. Ehret-Sabatier, I. Schalk and M. Harel, *Proc. Natl. Acad. Sci. U. S. A.*, 1993, **90**, 9031.
- 40 28 Y.-P. Pang and A. P. Kozikowski, *J. Comput.-Aided Mol. Des.*, 1994, **8**, 669.
- 45 29 E. H. Rydberg, B. Brumshtein, H. M. Greenblatt, D. M. Wong, D. Shaya, L. D. Williams, P.-R. Carlier, Y.-P. Pang, I. Silman and J. L. Sussman, *J. Med. Chem.*, 2006, **49**, 5491.
- 50 30 Y.-P. Pang, P. Quiram, T. Jelacic, F. Hong and S. Brimijoin, *J. Biol. Chem.*, 1996, **271**, 23646.
- 55 31 B. Svobodova, E. Mezeiova, V. Hepnarova, M. Hrabnova, L. Muckova, T. Koblrova, D. Jun, O. Soukup, M. L. Jimeno, J. Marco-Contelles and J. Korabecny, *Biomolecules*, 2019, **9**, 379.
- 32 (a) M. Kozurkova, S. Hamulakova, Z. Gazova, H. Paulikova and P. Kristian, *Pharmaceuticals*, 2011, **4**, 382; (b) M. Girek and P. Szymański, *Chem. Pap.*, 2019, **73**, 269.
- 33 (a) S.-S. Xie, X.-B. Wang, J.-Y. Li, L. Yang and L.-Y. Kong, *Eur. J. Med. Chem.*, 2013, **64**, 540; (b) L. Wang, I. Moraleda, I. Iriepa, A. Romero, F. López-Muñoz, M. Chioua, T. Inokuchi, M. Bartolini and J. Marco-Contelles, *MedChemCommun.*, 2017, **8**, 1307.
- 5 34 K. Oukoloff, N. Coquelle, M. Bartolini, M. Naldi, R. Le Guevel, S. Bach, B. Josselin, S. Ruchaud, M. Catto, L. Pisani, N. Denora, R. M. Iacobazzi, I. Silman, J. L. Sussman, F. Buron, J.-P. Colletier, L. Jean, S. Routier and P.-Y. Renard, *Eur. J. Med. Chem.*, 2019, **168**, 58.
- 10 35 S. Agatonovic-Kustrin, C. Kettle and D. W. Morton, *Biomed. Pharmacother.*, 2018, **106**, 553.
- 15 36 F. Mao, J. Li, H. Wei, L. Huang and X. Li, *J. Enzyme Inhib. Med. Chem.*, 2015, **30**, 995.
- 20 37 (a) N. Asano, *Curr. Top. Med. Chem.*, 2003, **3**, 471; (b) M. Bols, Ó. López and F. Ortega-Caballero, Inhibitors: structure, activity, synthesis, and medical relevance, in *Comprehensive glycoscience: from Chemistry to systems Biology*, ed. J. P. Kamerling, Elsevier Science, 2007, vol. 3, pp. 815–884; (c) C. Dehoux-Baudoin and Y. Génisson, *Eur. J. Org. Chem.*, 2019, 4765.
- 25 38 (a) N. Asano, R. J. Nash, R. J. Molyneux and G. W. J. Fleet, *Tetrahedron: Asymmetry*, 2000, **11**, 1645; (b) Ó. López, P. Merino-Montiel, S. Martos and A. González-Benjumea, Glycosidase inhibitors: versatile tools in Glycobiology, in *Carbohydrate Chemistry—Chemical and Biological approaches*, ed. A. P. Rauter and T. Lindhorst, RSC, 2012, vol. 38, pp. 215–262.
- 30 39 S. Sugimoto, H. Nakajima, K. Kosaka and H. Hosoi, *Nutr. Metab.*, 2015, **12**, 1.
- 35 40 J. Stirnemann, N. Belmatoug, F. Camou, C. Serratrice, R. Froissart, C. Caillaud, T. Levade, L. Astudillo, J. Serratrice, A. Brassier, C. Rose, T. Billette de Villemeur and M. G. Berger, *Int. J. Mol. Sci.*, 2017, **18**, E441.
- 40 41 G. Sunder-Plassmann, R. Schiffmann and K. Nicholls, *Expert Opin. Orphan Drugs*, 2018, **6**, 301.
- 45 42 (a) C. Decroocq, F. Stauffert, O. Pamlanrd, F. Oulaïdi, E. Gallienne, E. O. R. Martine, C. Guillou and P. Compain, *Bioorg. Med. Chem. Lett.*, 2015, **25**, 830; (b) J. I. Olsen, G. B. Plata, J. M. Padrón, Ó. López, M. Bols and J. G. Fernández-Bolaños, *Eur. J. Med. Chem.*, 2016, **123**, 155; (c) A. I. Ahuja-Casarín, P. Merino-Montiel, J. L. Vega-Baez, S. Montiel-Smith, M. X. Fernandes, I. Lagunes, I. Maya, J. M. Padrón, Ó. López and J. G. Fernández-Bolaños, *J. Enzyme Inhib. Med. Chem.*, 2021, **36**, 138.
- 50 43 H. H. Jensen, L. Lyngbye, A. Jensen and M. Bols, *Chem. – Eur. J.*, 2002, **8**, 1218.
- 55 44 M. P. Dale, H. E. Ensley, K. Kern, K. A. R. Sastry and L. D. Byers, *Biochemistry*, 1985, **24**, 3530.
- 45 Z. Najafi, M. Mahdavic, M. Saeedid, E. Karimpour-Razkenari, N. Edrakif, M. Sharifzadeh, M. Khanavi and T. Akbarzadeh, *Bioorg. Chem.*, 2019, **83**, 303.
- 46 S.-Y. Li, X.-B. Wang, S.-S. Xie, N. Jiang, K. D. G. Wang, H.-Q. Yao, H.-B. Sun and L.-Y. Kong, *Eur. J. Med. Chem.*, 2013, **69**, 632.

1 47 E. Riazimontazera, H. Sadeghpour, H. Nadri, A. Sakhteman, T. Tüylü Küçükkılınc, R. Miri and N. Edrakid, *Bioorg. Chem.*, 2019, **89**, 1.

5 48 E. Lindbäck, Ó. López, J. G. Fernández-Bolaños, S. P. A. Sauer and M. Bols, *Org. Lett.*, 2011, **13**, 2908.

10 49 N. Ardes-Guisot, D. S. Alonzi, G. Reinkensmeier, T. D. Butters, C. F. Becq, Y. Shimada, S. Nakagawa, A. Kato, Y. Bleriot, M. Sollogoub and B. Vauzeilles, *Org. Biomol. Chem.*, 2011, **9**, 5373.

15 50 F. Li, Z.-M. Wang, J.-J. Wu, J. Wang, S.-S. Xie, J.-S. Lan, W. Xu, L.-Y. Kong and X.-B. Wang, *J. Enzyme Inhib. Med. Chem.*, 2016, **31**, 41.

20 51 M. F. Snape, A. Misra, T. K. Murray, R. J. De Souza, J. L. Williams, A. J. Cross and A. R. Green, *Neuropharmacology*, 1999, **38**, 181.

25 52 G. Kryger, I. Silman and J. L. Sussman, *Structure*, 1999, **7**, 297.

30 53 J. K. Marquis, *Biochem. Pharmacol.*, 1990, **40**, 1071.

35 54 P. R. Carlier, E. S.-H. Chow, Y. Han, J. Liu, J. El Yazal and Y.-P. Pang, *J. Med. Chem.*, 1999, **42**, 4225.

40 55 T. M. Jespersen and M. Bols, *Tetrahedron*, 1994, **50**, 13449.

45 56 G. L. Ellman, K. D. Courtney, V. Andres, Jr. and R. M. Feather-Stone, *Biochem. Pharmacol.*, 1961, **7**, 88.

50 57 A. Cornish-Bowden, *Biochem. J.*, 1974, **137**, 143.

55 58 Y. Bourne, J. Grassi, P. E. Bougis and P. Marchot, *J. Biol. Chem.*, 1999, **274**, 30370.

60 59 W. Humphrey, A. Dalke and K. Schulten, *J. Mol. Graphics*, 1996, **14**, 33.

65 60 M. C. Desai, P. F. Thadeio, C. A. Lipinski, D. R. Liston, R. W. Spencer and I. H. Williams, *Bioorg. Med. Chem. Lett.*, 1991, **1**, 411.

70 61 J. P. B. Lopes, J. S. da Costa, M. A. Ceschi, C. A. S. Gonçalves, E. L. Konrath, A. L. M. Karl, I. A. Guedesd and L. E. Dardenne, *J. Braz. Chem. Soc.*, 2017, **28**, 2218.

75 62 M. J. Frisch, G. W. Trucks, H. B. Schlegel, G. E. Scuseria, M. A. Robb, J. R. Cheeseman, G. Scalmani, V. Barone, G. A. Petersson, H. Nakatsuji, X. Li, M. Caricato, A. V. Marenich, J. Bloino, B. G. Janesko, R. Gomperts, B. Mennucci, H. P. Hratchian, J. V. Ortiz, A. F. Izmaylov, J. L. Sonnenberg, D. Williams-Young, F. Ding, F. Lipparini, F. Egidi, J. Goings, B. Peng, A. Petrone, T. Henderson, D. Ranasinghe, V. G. Zakrzewski, J. Gao, N. Rega, G. Zheng, W. Liang, M. Hada, M. Ehara, K. Toyota, R. Fukuda, J. Hasegawa, M. Ishida, T. Nakajima, Y. Honda, O. Kitao, H. Nakai, T. Vreven, K. Throssell, J. A. Montgomery, Jr., J. E. Peralta, F. Ogliaro, M. J. Bearpark, J. J. Heyd, E. N. Brothers, K. N. Kudin, V. N. Staroverov, T. A. Keith, R. Kobayashi, J. Normand, K. Raghavachari, A. P. Rendell, J. C. Burant, S. S. Iyengar, J. Tomasi, M. Cossi, J. M. Millam, M. Klene, C. Adamo, R. Cammi, J. W. Ochterski, R. L. Martin, K. Morokuma, O. Farkas, J. B. Foresman and D. J. Fox, Gaussian, Inc., Wallingford CT, 2016.

80 63 J. Wang, R. M. Wolf, J. W. Caldwell, P. A. Kollman and D. A. Case, *J. Comput. Chem.*, 2004, **25**, 1157.

85 64 J. Wang, W. Wang, P. A. Kollman and D. A. Case, *J. Mol. Graphics Modell.*, 2006, **25**, 247260.

90 65 O. Trott and A. J. Olson, *J. Comput. Chem.*, 2010, **31**, 455.

95 66 J. A. Maier, C. Martinez, K. Kasavajhala, Koushik, L. Wickstrom, K. E. Hauser and C. Simmerling, *Chem. Theor. Comput.*, 2015, **11**, 3696.

100 67 W. L. Jorgensen, J. Chandrasekhar and J. D. Madura, *J. Chem. Phys.*, 1983, **79**, 926.

105 68 G. Bussi, D. Donadio and M. Parrinello, *J. Chem. Phys.*, 2007, **126**, 014101.

110 69 (a) M. J. Abraham, T. Murtola, R. Schulz, S. Páll, J. C. Smith, B. Hess and E. Lindahl, *SoftwareX*, 2015, **12**, 19–25; (b) D. van der Spoel, E. Lindahl, B. Hess, G. Groenhof, A. E. Mark and H. J. C. Berendsen, *J. Comput. Chem.*, 2005, **26**, 1701.

115 70 M. F. Sanner, *J. Mol. Graphics Modell.*, 1999, **17**, 57.